

9. SITE 542: TOE OF THE BARBADOS RIDGE COMPLEX¹

Shipboard Scientific Party²

HOLE 542

Date occupied: 21 February 1981

Date departed: 22 February 1981

Time on hole: 1 day, 11.2 hr.

Position: 15°31.2'N; 58°42.8'W

Water depth (sea level; corrected m, echo-sounding): 5016

Water depth (rig floor; corrected m, echo-sounding): 5026

Bottom felt (m, drill pipe): 5026

Penetration (m): 240

Number of cores: 7

Total length of core section (m): 66.50

Total core recovered (m): 52.56

Core recovery (%): 79.3

Oldest sediment cored:

Depth sub-bottom (m): 240

Nature: Ashy clays

Age: late Miocene (CN9)

Measured velocity (km/s): 1.679

Basement: Not reached

Number of cores: 12

Total length of core section (m): 114

Total core recovered (m): 90.22

Core recovery (%): 79.1

Oldest sediment cored:

Depth sub-bottom (m): 325

Nature: Scaly clays

Age: late Miocene

Measured velocity (km/s): 1.679

Basement: Not reached

HOLE 542B

Date occupied: 24 February 1981

Date departed: 27 February 1981

Time on hole: 3 days, 16.3 hr.

Position: 15°31.198'N; 58°42.793'W

Water depth (sea level; corrected m, echo-sounding): 5016

Water depth (rig floor; corrected m, echo-sounding): 5026

Bottom felt (m, drill pipe): 5026

Penetration (m): 323

Number of cores: None

Principal results: Hole 542 was spudded about 1.5 km landward of the deformation front of the Barbados Ridge complex. After washing and coring until 240 m, a 7.6° deviation of the drill string from the vertical required spudding of Hole 542A. Interval cores above 231 m and continuous coring from 231 to 325.5 m define a sequence of hemipelagic-pelagic Quaternary, Pliocene, and upper Miocene sediments. The cored section ranges from marly calcareous oozes (Unit 1) to clayey mudstones (Unit 2) with a concentration of ash beds in the lower Pliocene. Quaternary to uppermost Miocene calcareous muds were deposited between the lysocline and CCD (calcite compensation depth), whereas upper Miocene clays accumulated below the CCD.

The cored sequence is similar to those of the two tectonic units encountered at Site 541. A possible repetition of a nannofossil zone between 183 and 195 m suggests a small-scale reverse fault. From 250 m to the base of Hole 542A, cores show progressive development of fracturing and foliation comparable to what we observed at the bottom of Hole 541.

Dips (20–35°) observed in the cores below 200 m are steeper than dips (2°) of seismic reflectors below the discontinuously reflective unit. Apparently the discontinuously reflective unit is folded and faulted internally but overlies the seismically layered sequence along a décollement.

Hole 542A was abandoned due to collapse of fractured and sheared mudstones in a zone of probable excess pore water pressure. An attempt to case the sheared and fractured zone (Hole 542B) failed, although the stuck casing resulted in an inadvertent packer experiment suggesting lithostatic fluid pressure in the basal deformed zone. Site 542 was abandoned without penetration of the subducted sedimentary sequence.

BACKGROUND AND OBJECTIVES

Because of unstable hole conditions, Site 541, located at the toe of the Barbados Ridge complex (Fig. 1),

¹ Biju-Duval, B., Moore, J. C., et al., *Init. Repts DSDP*, 78A: Washington (U.S. Govt. Printing Office).

² Bernard Biju-Duval (Co-Chief Scientist), Institut Français du Pétrole, 92305 Rueil Malmaison, France (present address: Centre National pour l'Exploitation des Océans, 66 Avenue d'Iéna, 75116 Paris, France); J. Casey Moore (Co-Chief Scientist), Earth Sciences and Marine Studies, University of California at Santa Cruz, Santa Cruz, California; James A. Bergen, Department of Geology, Florida State University, Tallahassee, Florida; Grant Blackinton, Hawaii Institute of Geophysics, University of Hawaii at Manoa, Honolulu, Hawaii; George E. Claypool, Branch of Oil and Gas Resources, U.S. Geological Survey, Denver Federal Station, Denver, Colorado; Glenn Foss, Deep Sea Drilling Project, Scripps Institution of Oceanography, La Jolla, California; Rodolfo T. Guerra, Exploration Services Center, Mobil Exploration and Producing Services, Dallas, Texas; Christoph H. J. Hemleben, Institut und Museum für Geologie und Paläontologie, Universität Tübingen, D-7400 Tübingen 10, Federal Republic of Germany; Michael S. Marlow, U.S. Geological Survey, Menlo Park, California; James H. Natland, Deep Sea Drilling Project, Scripps Institution of Oceanography, La Jolla, California; Carol J. Pudsey, Department of Geology, University of Leicester, Leicester, United Kingdom; G. W. Renz, Deep Sea Drilling Project, Scripps Institution of Oceanography, La Jolla, California (present address: 5260 Angeles Crest, La Canada, California); Marc Tardy, Département de Sciences de la Terre, Université de Savoie, BP 1104, Chambéry, France; Douglas Wilson, Hawaii Institute of Geophysics, University of Hawaii at Manoa, Honolulu, Hawaii (present address: Department of Geophysics, Stanford University, Stanford, California); Audrey Wright, Earth Sciences and Marine Studies, University of California at Santa Cruz, Santa Cruz, California (present address: Deep Sea Drilling Project, Scripps Institution of Oceanography, La Jolla, California).

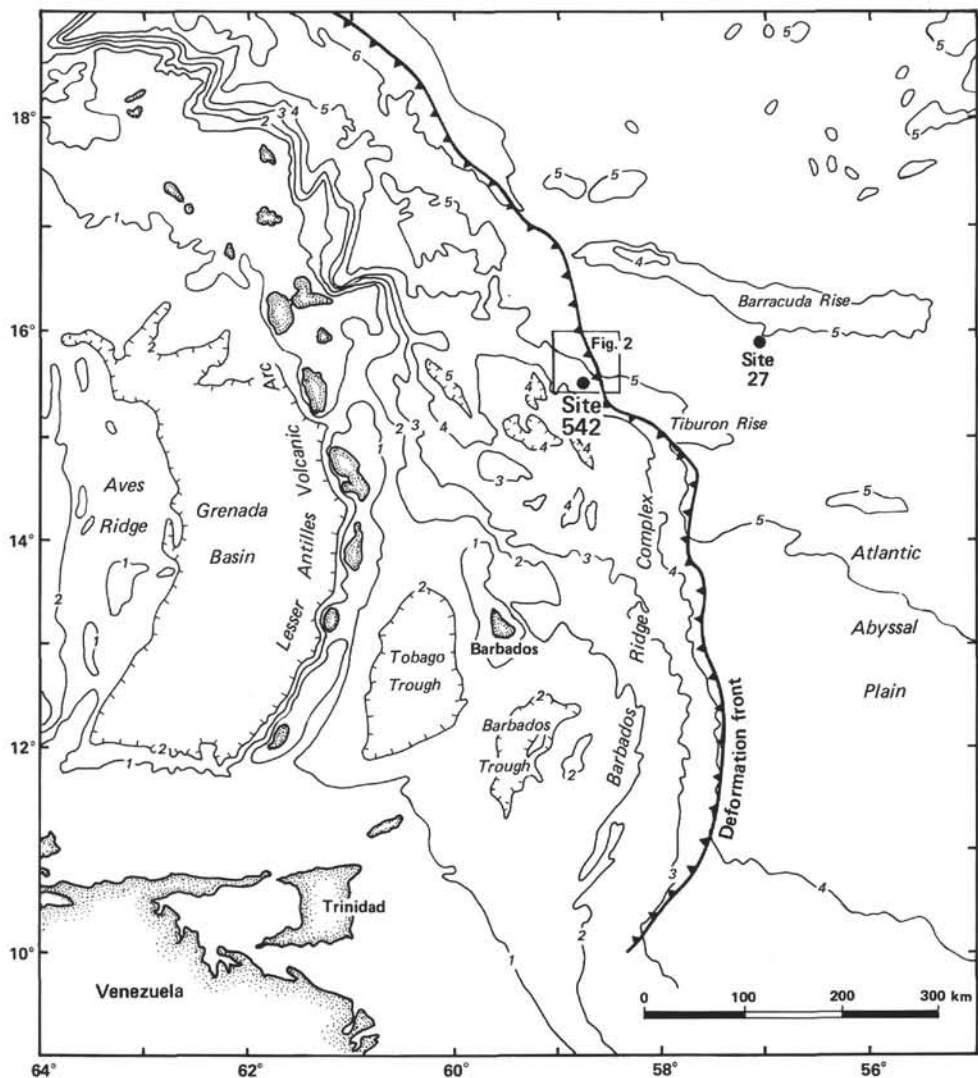


Figure 1. Barbados Ridge complex, general location map (contour intervals are in kilometers.)

had to be abandoned when the main shear zone between the discontinuously reflective sequence and undisturbed sediments was penetrated; only a part of the drilling objectives were thus accomplished. At Site 541, for the first time in DSDP history, the superposition of two off-scraped tectonic units was clearly documented; nevertheless, the possibly underthrust sediments underlying the down-going ocean crust of the Atlantic were not significantly penetrated. Moreover, the scheduled emplacement of a downhole seismometer and tiltmeter in the ocean crust was not completed. In order to attain these other objectives we attempted to drill another hole seaward, between Site 541 and the toe of the Barbados Ridge complex. Successful completion of drilling at Site 542 would have permitted clear definition of the shear zone between the off-scraped and underthrust sequences and revealed the stratigraphic, structural, and diagenetic history of the underthrust sequence.

The location of Site 542 (Figs. 2 and 3), based on profile A1D, was selected to minimize the sub-bottom depth of the shear zone (380 m/s two-way traveltime, see Fig. 3) and make it possible to reach the basement at

about 1.0 s sub-bottom. Our drilling program called for washing (with only two reference cores at 80 and 150 m in order to obtain information on lithology, physical properties, and geochemistry). Continuous coring was scheduled from 200 m sub-bottom to the basement.

Specific objectives at Site 542 were: (1) to establish the type of contact between the acoustically chaotic units and the layered undergoing sediments, and to define the structural geology and physical properties of this shear zone near the tow of the Ridge; (2) to date and establish the lithology and structural nature of the layered sequence; (3) to date the ocean crust underthrusting the deformation front; and (4) to emplace a downhole seismometer and tiltmeter into the ocean crust.

OPERATIONS

Hole 542

The second drill site was selected about 1.5 km seaward of Site 541 where the seismic reflector believed to represent the décollement zone could be traced to a shal-

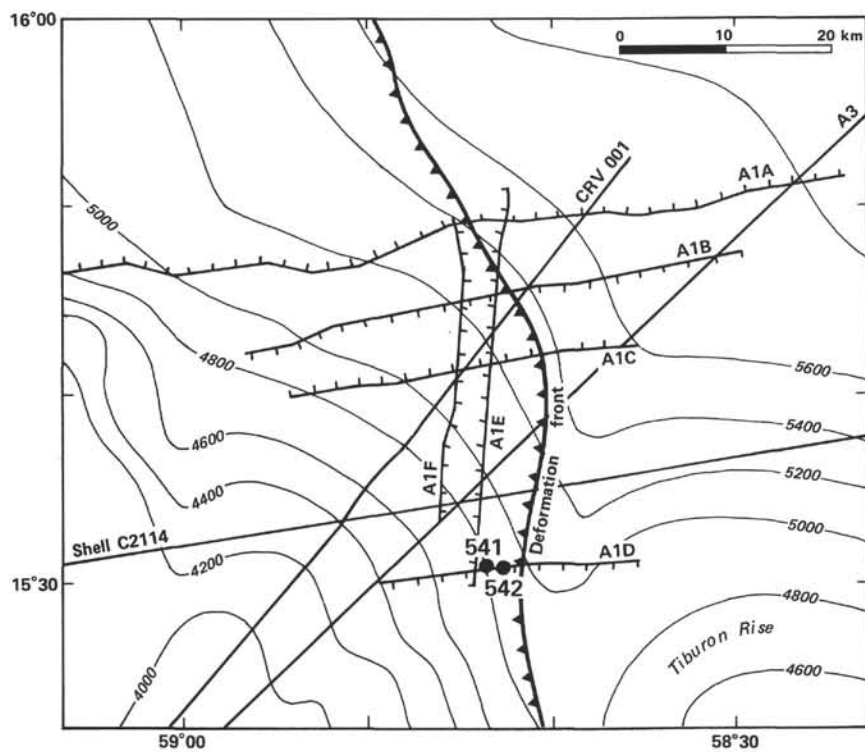


Figure 2. Site 542 location map (box, Fig. 1). (Note position of deformation front and seismic reflection lines A1A–A1D from the IFP/CNEXO seismic site survey [from Ngokwey et al., this volume]. Bathymetry is in meters.)

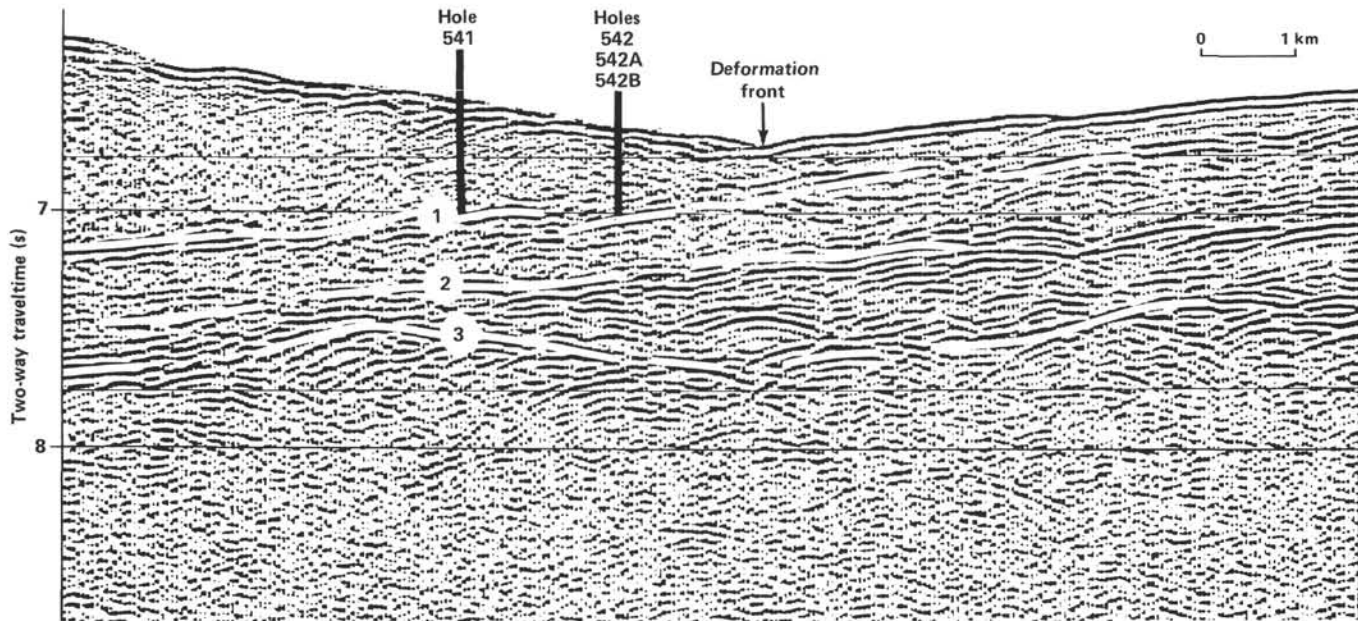


Figure 3. Seismic reflection line A1D (IFP/CNEXO survey, Ngokwey et al., this volume) with the locations of Sites 541 and 542. (Reflector 1: prominent reflector, top of the undisturbed sediments; Reflector 2: prominent reflector in the underthrusting sedimentary sequence; Reflector 3: ocean crust [top of layer 2].)

lower depth. Here we hoped that the less deeply buried clay would be deformed plastically and be less likely to cause drilling problems than the fractured claystone below 400 m in Hole 541. The vessel was moved by using offsets and by monitoring the position display of the dy-

namic positioning system. The new acoustic beacon was dropped only 34 min. after the move began. The position was refined by positioning system offsets during the ensuing pipe trip after reference profiles and satellite navigation fixes had been reviewed.

Hole 542 was spudded at 2321 hr., 21 February, after a 5-hr. delay caused by a malfunction in the Bowen power sub system.

The hole was drilled from the seafloor depth of 5026 to 202 m sub-bottom, with three "spot" or "wash" cores taken from the interval. These are designated Cores H1, H2 and H3, and each may have recovered material over the entire washed interval (39–79 m, depending on the core). Continuous coring then proceeded without incident to 240 m sub-bottom. Coring and recovery data are listed in Table 1. A routine drift measurement at this point indicated that the hole angle was 7.6° off vertical. This large deviation was undesirable and exceeded the acceptable angle for the downhole seismometer scheduled for implantation here. Consequently we abandoned Hole 542 and spudded Hole 542A in an attempt to drill more vertically. The bit was pulled clear of the seafloor at 1748 hr., 22 February.

Hole 542A

Hole 542A was spudded at the same location at 1823 hr., 22 February. We took two spot or wash cores (H1 and H2) from the drilled interval of 0 to 240 m sub-bottom. Core 1 was taken immediately below H1 between 173.5 and 183 m sub-bottom. A drift survey taken at 173.5 m showed an acceptable deviation of 2.3°.

Coring and recovery data for this hole as well are listed in Table 1. Continuous coring below H2 produced high core recovery with no hole problems until Core 7 (287.5–297 m sub-bottom). Recovery was low for this core and high pump pressure was noted as the next inner barrel was pumped into place. Three more cores were taken with progressively more hole fill and sticking tendencies, as in Hole 541, despite copious spotting of barite mud and flushes. When 25 m of hole fill were en-

countered following the retrieval of Core 10, we judged the conditions to be hopeless and terminated operations. The drill string was recovered, with the bit arriving on deck at 1030 hr., 24 February.

Hole 542B

The vessel was offset 30 m to the north to avoid the disturbed area of the two previous holes as preparations were made for a final attempt to penetrate the thrust fault plane and reach basement. We hoped to isolate the unstable fault zone behind a short length of casing attached to the BHA (bottom-hole assembly) and drilled into place opposite the fault zone. The casing would then be released and would remain in place while normal coring operations proceeded to total depth.

Fourteen hours were required to assemble the 57-m string of 11.75-in. casing with its special 17.5-in. drilling shoe and drive-hanger assembly (Fig. 4). This process included completely reconfiguring the BHA and attaching the casing to the BHA by means of a special lowering-drive sub. The ensuing pipe trip was routine, and Hole 542B was spudded at 1037 hr., 25 February.

We planned no cores until after release of the casing. Drilling proceeded to 110.5 m sub-bottom where, with the BHA safely buried, a deviation survey indicated an acceptable hole angle of 0.6°. We noted higher torque and a lower penetration rate than usual, as expected, due to the 17.5-in.-diameter drilling shoe. However, no drilling problems occurred during the 15.75 hr. required to drill the casing to a depth of 323.5 m sub-bottom.

We then raised the drill string to bring a tool joint to the rig floor so that the pipe could be broken to introduce the inner core barrel carrying the shifting tool. Due to a misunderstanding, the pipe was raised to the second tool joint (as in standard coring procedure) instead of the intended 4 m to the first tool joint. With the shifting tool in the string, the pipe was made up and found to be stuck, both vertically and rotationally. Simultaneously we noted that the drill pipe pressure had jumped from 0 to over 300 psi. At this point, the drilling shoe (at 310 m sub-bottom) was about 10 m below the (estimated?) fault zone.

The shifting tool was lowered into the BHA and then pulled upward, engaging the internal sleeve of the lowering sub. The sleeve was stuck and could not be shifted upward. As the shifting mechanism is designed to release only after the sleeve had reached its full travel, it was necessary to pull and "work" the wire line until safety shear pins at one of two locations failed, releasing the wire-line assembly. In this instance, pivot pins on two of the shifting tool dogs sheared and the entire shifting tool assembly was recovered. During three additional wire-line runs and shifting attempts, the overshot shear pin failed, leaving the inner barrel/shifting tool assembly in the pipe.

When hopes of releasing the casing string had faded, we attempted to free the casing and recover the entire drill string. The casing could only be raised 4 m, returning to its original position without difficulty; 25 min. of "working" failed to move it farther or to achieve rotation. Remarkably, the ability to circulate had never been

Table 1. Coring summary Site 542.

Core no.	Date (Feb. 1981)	Time	Depth from drill floor (m) top bottom	Depth below seafloor (m) top bottom	Length cored (m)	Length recovered (m)	Amount recovered (%)
Hole 542							
H1 ^a	22	0226	5026.0–5114.0	0–88.0	—	4.29	—
H2 ^a	22	0540	5114.0–5180.5	88.0–154.5	—	6.56	—
H3 ^a	22	0802	5180.5–5228.0	154.5–202.0	—	6.37	—
1	22	0940	5228.0–5237.5	202.0–211.5	9.5	9.56	101
2	22	1155	5237.5–5247.0	211.5–211.0	9.5	8.20	86
3	22	1330	5247.0–5256.5	221.0–230.5	9.5	8.17	86
4	22	1602	5256.5–5266.0	230.5–240.0	9.5	9.41	99
Total				66.5	52.6	79	
Hole 542A							
H1 ^a	22	2300	5026.0–5199.5	0–173.5	7.58	7.58	—
1	23	0053	5199.5–5209.0	173.5–183.0	9.5	7.31	77
H2 ^a	25	0345	5209.0–5266.0	183.0–240.0	9.39	9.39	—
2	25	0512	5266.0–5275.5	240.0–249.5	9.5	10.03	105
3	23	0657	5275.5–5285.0	249.5–259.0	9.5	8.59	90
4	23	0827	5285.0–5294.5	259.0–268.5	9.5	7.66	81
5	23	1035	5294.5–5304.0	268.5–278.0	9.5	9.71	102
6	23	1232	5304.0–5313.5	278.0–287.5	9.5	8.59	90
7	23	1415	5313.5–5323.0	287.5–297.0	9.5	3.73	39
8	23	1628	5323.0–5332.5	297.0–306.5	9.5	7.94	84
9	23	1945	5332.5–5342.0	306.5–316.0	9.5	2.46	26
10	23	2315	5342.0–5351.5	316.0–325.5	9.5	7.19	76
Total				114.0	90.0	79	

Note: No cores were recovered from Hole 542B.

^a Cores 542-H1, -H2, and -H3, and 542A-H1 and -H2 are wash cores in which drilling penetrated more than the standard 9.5 m. Material recovered in these cores can thus be from any location in the cored interval. Percent recovery data are not given for these cores.

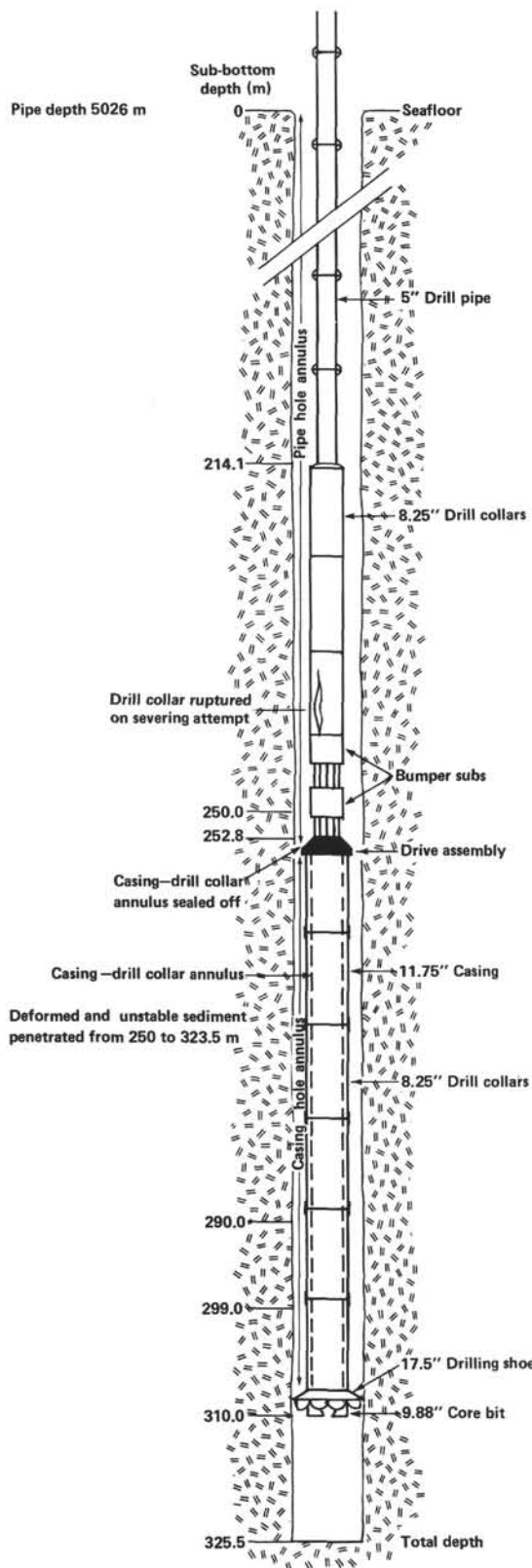


Figure 4. Schematic of downhole hardware used in Hole 542B. (Deformed and unstable sediment apparently collapsed into the hole causing sticking of casing and packing-off of hole, which apparently isolated the base of the hole and allowed high fluid pressure to be measured through the drill pipe. A thrust fault probably lies in the zone of deformed and unstable sediment.)

lost, although pump pressures were a few hundred psi higher than normal.

At this point a primacord wire-line severing charge was rigged and run down the pipe to the BHA. The intent was to sever the drill string in the bumper sub just above the casing lowering sub and thereby recover the upper part of the BHA. Depth control for placement of the severing charge was uncertain, owing to several factors; we later calculated that the first charge was fired in a drill collar. The drill string failed to part when the shot was fired, although, as recorded at the driller's console, the pipe pressure dropped sharply from a static 350 psi to 0.

The only plausible explanation for this phenomenon was that the severing charge had ruptured the drill string and that water was flowing from the geopressured lower part of the hole, up through the pipe, and out into the pipe-hole annulus. The casing-hole annulus had apparently become packed off above the pressured zone at the time the casing became stuck in the hole. Two additional attempts were then made to sever the drill string, but both charges failed to detonate due to faulty blasting caps.

At this time a through-pipe temperature log was run in an attempt to document the flow of water into the hole. If, as at Site 541, relatively warm water was flowing up the hole, it could produce a fairly constant anomalously high temperature for the entire borehole. The log recorded a normal-appearing (though somewhat high) temperature gradient for the hole, which indicated that the core bit or lower BHA may have become plugged off, thereby stopping the flow, or that the flow of water from the lower portion of the hole may not have been anomalously warm. This possibility was supported by the fact that sediment-cuttings fill had been encountered at progressively higher points in the BHA on successive severing attempts.

A severing charge was then lowered for the fourth time and fired successfully to part the string in the drill pipe above the BHA. The remainder of the drill string was then recovered, with all pipe on deck at 0215 hr., 28 February.

SEDIMENT LITHOLOGY

Lithostratigraphy

Site 542 is located at 5016 m water depth, about 1.5 km west of the toe of the accretionary prism. Two holes that recovered cores were drilled at Site 542, Holes 542 and 542A (Fig. 5). Hole 542 was abandoned at a sub-bottom depth of 240 m because the deviation of the hole angle from vertical was unacceptable. Hole 542A collapsed at a sub-bottom depth of 325.5 m.

Neither hole was cored continuously through the entire section drilled. Hole 542 was cored continuously below 202 m; Hole 542A was cored continuously below 240 m. Several wash cores were taken from the top section of each hole to monitor gross lithologic and biostratigraphic changes downhole for comparison with Site 541.

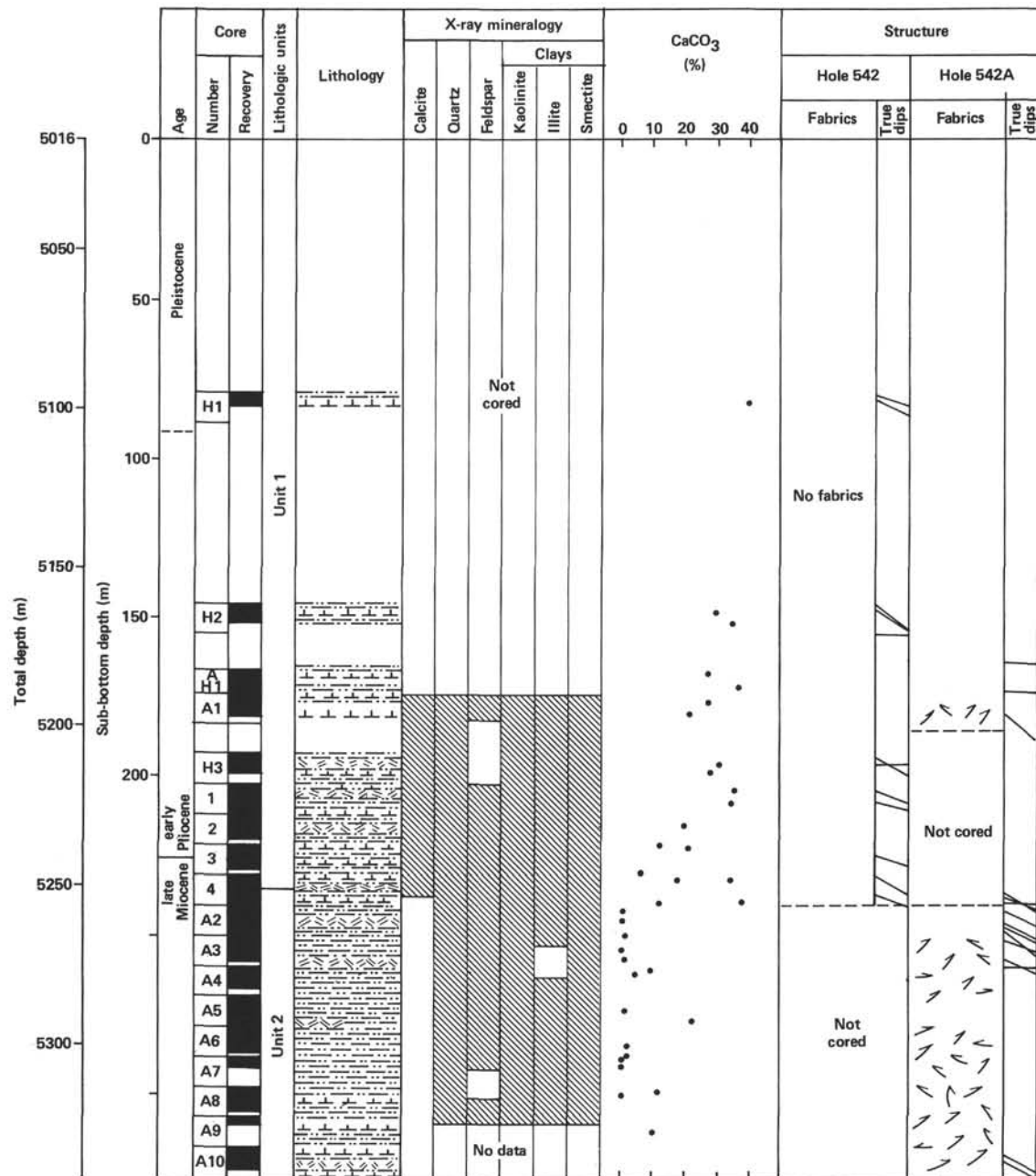


Figure 5. Summary lithology, sediment composition, structure, physical properties, and seismic stratigraphy, Site 542. (Hole 542A cores are denoted by prefix A. Wash core 542A-H2 is not shown because it is overlapped by Hole 542 cores. In X-ray Mineralogy column, blackened areas show presence.)

On the basis of macroscopic core descriptions, smear slide analyses, and carbonate bomb data, the sediments at Site 542 can be divided into two lithostratigraphic units. A summary of these units is shown in Table 2. Carbonate percentages found downhole at Site 542 were determined with the shipboard carbonate bomb (Fig. 5).

Lithologic Unit 1 is a 240-m thick, bioturbated, lower Pleistocene- to- upper Miocene marly foraminifer-nannofossil ooze or marly nannofossil ooze (containing thin ash layers, ash patches, and dispersed ash particles). Ash was found in every core drilled at Hole 542 and in the uppermost three cores of Hole 542A. The

unit is light gray (5Y 6/1) to olive gray (5Y 5/2) in the uppermost part of the unit, gradually changing to grayish brown (2.5Y 5.2) or light brownish gray (2.5Y 6/2) below 210 m. This color change corresponds to an increasing clay content downsection. The ash layers and patches are dark gray (N4) to very dark gray (N3) to black and commonly are flanked by light bluish gray (5B 7/1) or green gray (5G 6/1) alteration zones. The entire unit has been moderately deformed by drilling. It is in conformable contact with underlying Unit 2.

Lithologic Unit 2 is a bioturbated, mottled, upper Miocene mud or ashy mud with thin layers of marly

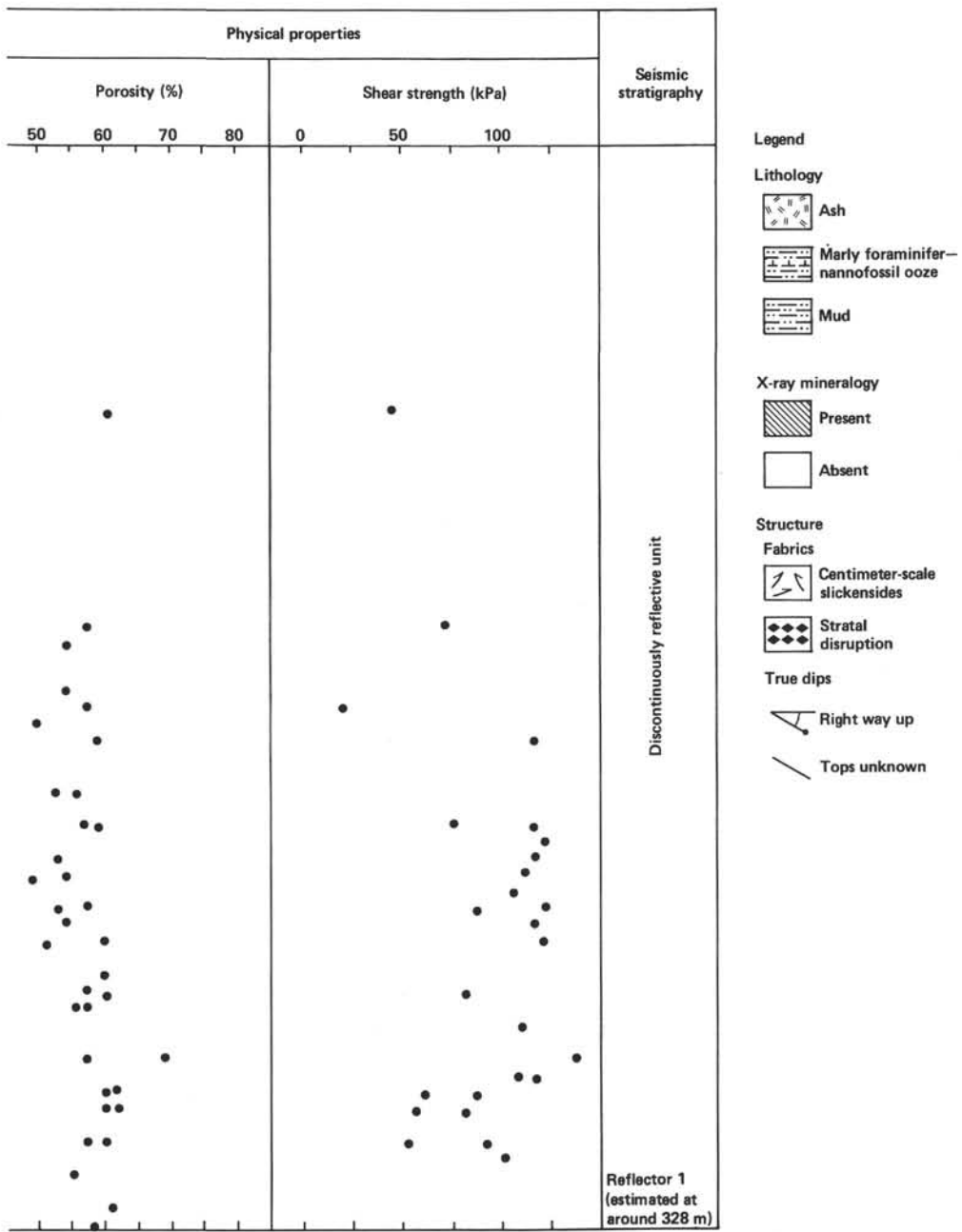


Figure 5. (Continued).

nannofossil ooze, thin ash beds, and dispersed ash particles. An absence or scarcity of calcareous components differentiates it from Unit 1. Unit 2 is dominantly greenish gray (5GY 5/1) with common gray ashy mottles. The dark gray (N4) to very dark gray (N3) ash layers have been largely redistributed by burrowing and commonly have light green gray (5G 5/1 to 5G 6/1) alteration zones. The occurrence of infrequent, thin zones of marly nannofossil ooze suggests that the level of the CCD fluctuated during the time in which this unit was deposited, perhaps in association with late Miocene changes in worldwide oceanographic conditions. Much of the sediment cored in Unit 2 is internally deformed and is characterized by well-developed, slickensided fracture surfaces.

All of the sediments cored at Site 542 appear to have been deposited below the lysocline. Though some of the sediments may have been deposited by current action, the vast majority of them accumulated by pelagic-hemipelagic settling in a quiet, deep-water environment adjacent to the Lesser Antilles island arc. The selective fractionation of the foraminiferal assemblage observed in Sample 542-143-4, 30–40 cm (the interval consists of exclusively globular foraminifers overlain by a fine section of foraminifer fragments) indicates that the layer was deposited by some sort of sediment gravity flow. Ash from eruptions along the island arc settled to the seafloor and was subsequently redistributed by burrowing organisms. The lack of terrigenous turbidites in the cored section suggests that the location of the site was

Table 2. Lithologic units, Site 542.

Lithostratigraphic unit	Lithology	Cores		Sub-bottom depth (m)	
		Hole 542	Hole 542A	Hole 542	Hole 542A
1	Ashy, marly foraminifer-nan-nanofossil ooze and ash, marly nannofossil ooze with thin ash layers	H1-H3; 1-4, Section 3	H1, 1, H2	0-235.0	0-240
2	Mud or ash mud with thin layers of marly nannofossil ooze and thin layers of ash	4, Section 3-end of Core 4	2-10	235.0-240	240-325.5

on a topographic high or, less likely, a great distance from any terrigenous source.

Comparison of the sediments of Unit 1, Site 542 with Lithologic Units 1 to 3 and 5, Site 541 indicates similar age and lithology. Likewise, Unit 2 at Site 542 is comparable in age and lithology to Lithologic Units 4 and 6 at Site 541 (Table 3). Although the two units drilled at Site 542 probably correlate with their similar counterparts at Site 541, it is uncertain whether Tectonic Unit A or B (see Site 541 report) is more closely represented by the cores drilled at Site 542. Comparison with seismic stratigraphy and structural data allow us to propose tentative correlation of Units 1 and 2 at Site 542 with Tectonic Unit B at Site 541.

Bioturbation

All the cores from Hole 542 show indistinct burrow mottling, rarely of recognizable *Planolites* and *Chondrites* type. Hollow *Cylindrichnus* was found at the base of a dark gray ash in Core 1, Section 3, and a *Zoophycus* at the top of Core 2, Section 5.

In Hole 542A burrow mottling is again ubiquitous but mostly indistinct. Core 3, Section 3 contains a near-horizontal, *Zoophycus*-related burrow (*Lophoctenium*?), which differs from *Zoophycus* in that the burrow traces touch each other (Fig. 6A). Immediately below this burrow is a tiny *Chondrites* system with individual burrows only 0.5 mm in diameter. Core 4 contains abundant *Zoophycus*, including a notable example at the top of Section 5 (Fig. 6B). This sample shows seven whorls and faint traces of the axis of the corkscrewlke trace: the whorl system is smaller than usual (commonly whorls extend right across the core and are about 4 mm thick), so it may have been made by a juvenile *Zoophycus*. Significantly the whorl system is not parallel to the core axis but inclined at 30°. Because *Zoophycus* is be-

lieved to create a vertical corkscrew burrow, this gives a structural dip of 30°.

The remaining cores from Hole 542A (Cores 5-10) are burrow mottled with no recognizable ichnogenera.

X-Ray Mineralogy

Eighteen samples were analyzed from this site, using the same method as described in the Site 541 report. The same minerals—quartz, alkali feldspar and plagioclase, calcite, kaolinite, illite, and smectite—were identified. Their proportions, estimated very roughly from peak heights, vary in a similar fashion to those at Site 541. Results are summarized in Figure 5. Quartz is present in all samples and shows no systematic increase or decrease down the hole. One or both feldspars are present in most samples, but there is little feldspar from 180 to 250 m. Calcite is present in the Pliocene part of the section down to 240 m sub-bottom. Kaolinite, illite, and smectite are present in (very) approximately equal proportions down to 255 m, where smectite increases at the expense of illite. Again, this smectitic interval corresponds to particularly fractured clays.

Volcanic Ash

A total of 46 ash beds were recovered at Site 542, 18 in Hole 542, and 28 in Hole 542A. Of these, 13 are major ash falls 2 to 12 cm thick, three of which occur in units that correlate in time and depth in the two holes. There are therefore 9 major ash beds in Hole 542 and 1 in Hole 542A that do not repeat. Of these, eight are lower Pliocene and two upper Miocene. These therefore belong to the mostly lower Pliocene pulse of major explosive magmatism that was documented for the Lesser Antilles arc in Hole 541. Details of the correlations can be found in the chapter on volcanic ash by Natland (this volume).

STRUCTURAL GEOLOGY

Structural features and attitudes of Holes 542 and 542A are graphically depicted in a structure log presented in Figure 5 (see also Cowan et al., this volume). We did not see any small-scale structures in cores from the Hole 542. We measured 13 attitudes in these cores ranging from horizontal to 38° and averaging 16°. Attitudes of 12°, 18°, and 30° in Cores 3 and 4 are suspect, however, because the hole was deviating 7.6° in this interval. As at Site 541, horizontal layers were noted below gently dipping layers in Cores H2 and H3. We believe these anomalies may be due to small displacements along faults that leave no other structural record of their exist-

Table 3. Correlation of lithologic units cored at Site 541 (Tectonic Units A and B) with those cored at Site 542.

Site 541 ^a		
Tectonic Unit A	Tectonic Unit B	Site 542 ^b
Lithologic Units 1, 2, and 3: Recent to late Miocene calcareous muds and marly calcareous oozes	Lithologic Unit 5: → Pliocene to late Miocene calcareous muds	Lithologic Unit 1: → Recent to late Miocene marly calcareous oozes
Lithologic Unit 4: late Miocene muds	Lithologic Unit 6: → late Miocene to middle Miocene mudstones	Lithologic Unit 2: → late Miocene muds
—	Lithologic Unit 7: early Miocene radiolarian mudstones	—

^a See Site 541 (this volume) for detailed descriptions of lithologic units enumerated here.

^b Detailed descriptions of Site 542 lithologic units are given in the sediment Lithology section of this chapter.

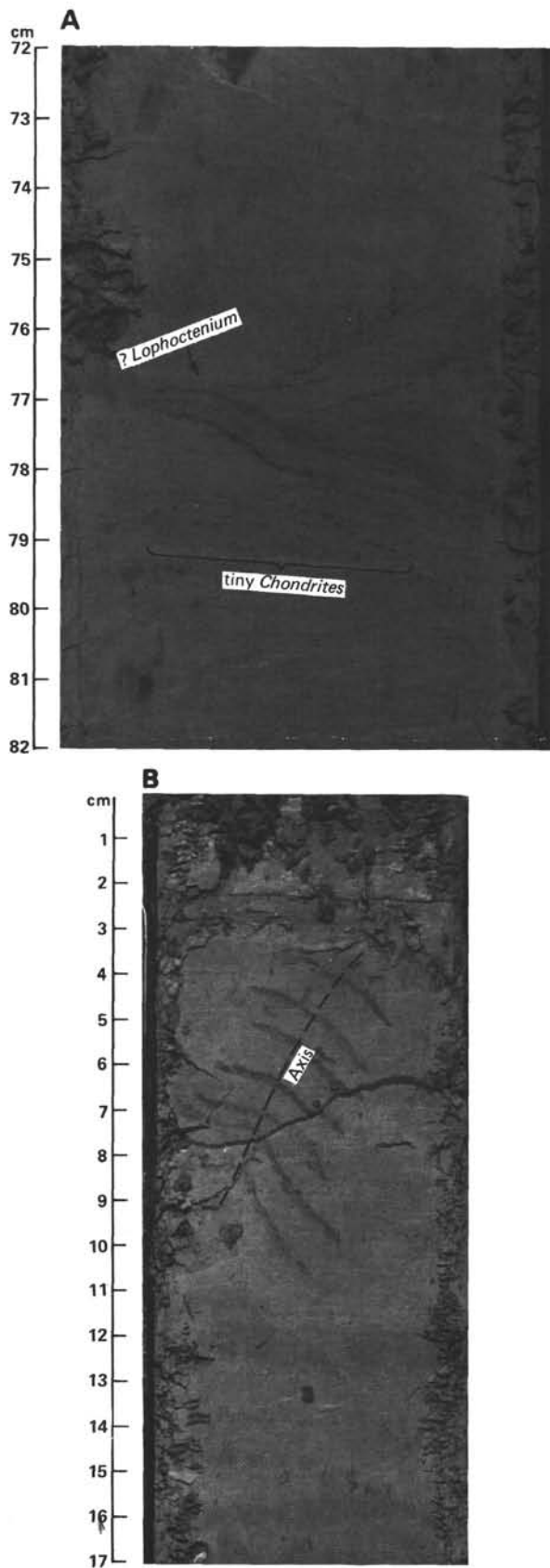


Figure 6. A. *Lophocentrum*-like burrows and tiny *Chondrites* system in 542A-3-3, 72–82 cm. B. Complete small *Zoophycus* spiral in 542A-4-5, 0–17 cm. (Axis of spiral inclined at 30° to core.)

ence. Possible evidence for such displacements is that a nannoplanktonic zonal marker occurs approximately 30 m deeper in Hole 542 than in Hole 542A (see the Biostratigraphy section, this chapter).

In Hole 542A, dips range from horizontal to 40°; the average of 15 attitudes, 6 of them known to be right-way-up, is 17°. Much of the section below Core 3 (249.5 m) displays semipenetrative internal deformation recorded by randomly oriented, polished surfaces spaced 1 or 2 mm to 1 cm apart. These structures generally are not apparent on cut surfaces of cores except as irregular, thin (1–2 mm), anastomosing discontinuities in Core 3, Section 5, but are evident when pieces of sticky coherent mud are broken apart. A similar fabric is present in Cores 25 to 30 at Site 541. These features are small-scale slip surfaces along which part of an overall, mesoscopically ductile flow was accommodated. Other evidence for internal flow is stretched bioturbation burrows and mottles, which are prominent in Sections 5 and 6 of Core 6 and Sections 4 and 5 of Core 8. Also Core 5, Section 3 (31–62 cm) is reminiscent of Cores 28 to 30 at Site 541. Irregularly elongate, distorted bands of differently colored mud, presumably representing original layers, have been deformed and probably disrupted and are presently separated by steeply dipping contacts that subsequently were offset and rotated along horizontal drilling fractures.

Any given section of core below about 250 m in Hole 542A typically contains both deformed and undeformed intervals, and it was impractical to differentiate these section by section either in our core descriptions or in Figure 5. In comparison with Cores 25 to 30 at Site 541, the polished, slickensided surfaces at Hole 542A are probably more closely spaced but are present in less of the cored sedimentary section. Perhaps they also record internal, plastic deformation associated with faulting, although no age reversals or repeated stratigraphy was detected in Hole 542A. As at Site 541, smectite is more abundant in deformed muds below about 250 m. Independent evidence for faulting may include: (1) poor recovery in Cores 7 and 9; (2) general deterioration in hole conditions at and below Core 7, which ultimately forced us to cease drilling Hole 542A; (3) odd, compact breccias in Core 7 of elongate to angular and equant fragments of cohesive mud, in a soft to soupy mud matrix, which may represent fragments from *in situ* breccias that accumulated in the hole and were cored subsequently; and (4) possibly high (approximately lithostatic) *in situ* fluid pressures at or below 300 m. These factors suggest that a fractured, permeable, overpressured fault zone was penetrated in Hole 542A. In fact, some fracture-induced enhancement of permeability in the partly consolidated, compacted, impermeable muds is required to allow a substantial flow of water into the hole in response to abnormally high fluid pressure. The absence of stratigraphic inversions points to layer-parallel (*décollement*) faulting facilitated by low (~0 psi) effective stress.

BIOSTRATIGRAPHY

A summary of the biostratigraphy of Site 542 for nannofossils and foraminifers is given in Figure 7. In

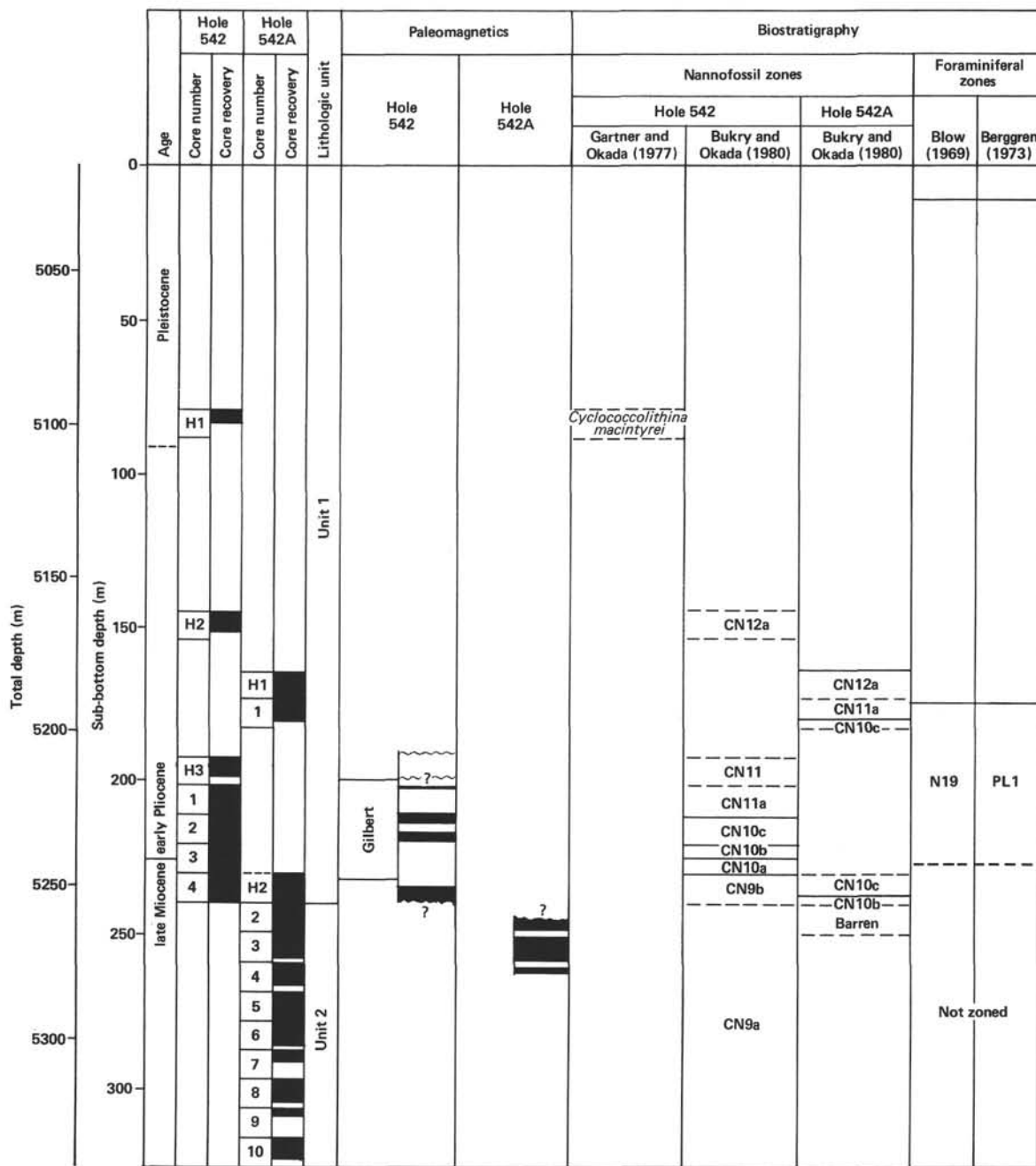


Figure 7. Summary of Site 542 biostratigraphy and magnetostratigraphy. (Polarity normal intervals are black, and polarity reversed intervals are white.)

this section, the basis of zonal assignments for each of these microfossil groups is discussed. The biostratigraphy described here is based on shipboard investigations. For a more complete summary of nannofossils see Bergen (this volume).

Nannofossils

Offset Sequences in Holes 542 and 542A

In Hole 542, the top of the *Ceratolithus rugosus* Sub-zone (CN10c) is placed at Sample 542-2-1, 61-62 cm, and is based on the extinction of *Amaurolithus tricorniculatus*. This datum occurs at approximately 212 m sub-

bottom in this hole. The top of the *Ceratolithus rugosus* Subzone (CN10c) is placed at Sample 542A-1-5, 58–59 cm in Hole 542A. The depth of this boundary in this hole is approximately 180 m. A difference of 30 m in depth for this datum between the two holes means that a portion of the section is repeated at Site 542.

Two small repetitions of section may occur in Hole 542A, Cores 3 through 10 (see Bergen, this volume).

Hole 542

This hole was washed to a depth of 202 m. The three washed cores were taken from that interval. Core H1 is placed in the *Cyclococcolithina macintyrei* Zone of Gart-

ner (1977). This is his lowermost zone in the Pleistocene, and is defined on the basis of the extinctions of *Discoaster brouwerii* and *Cyclococcolithina macintyreai*. Core H2 is placed in the upper Pliocene *Discoaster tamalis* Subzone (CN12a) of Bukry and Okada (1980). *Sphenolithus abies*, *S. neoabies*, and *Reticulofenestra pseudoumbilica* are all present throughout Core H3. This entire core is placed in the *Reticulofenestra pseudoumbilica* Zone (CN11). *Discoaster* is common in the top half of this core.

Four continuous cores were taken below 202 m. Core 1 is assigned to the lower Pliocene *Sphenolithus neoabies* Subzone (CN11a). *D. asymmetricus*, whose acme defines the top of this subzone, is very rare in this core. Core 2 is placed in the *Ceratolithus rugosus* Subzone (CN10c), based on the presence of *A. tricorniculatus* and the absence of *c. acutus*. *A. delicatus* is last observed in Sample 452-2-5, 96–97 cm. Core 3, Sections 1 through 3 is assigned to the *Ceratolithus acutus* Subzone (CN10b) based on the entire range of that species.

The *Triquetrorhabdus rugosus* Subzone (CN10a) is a gap zone between the last *D. quinqueramus* and first *C. acutus*. It is difficult to delineate in this hole because of the rare and sporadic occurrence of *D. quinqueramus* in Core 3. This lower boundary is therefore placed above the last consistent occurrence of *D. quinqueramus* in Sample 542-4-1, 27–28 cm. The presence of both *A. primus* and *D. quinqueramus* places all of Core 4 in the *Amaurolithus primus* Subzone (CN9b).

Hole 542A

Core H1 is placed in the *Discoaster tamalis* Subzone (CN12a) because of the presence of *Discoaster tamalis* and absence of *Reticulofenestra pseudoumbilica* and *Sphenolithus neoabies*. Core 1, Sections 1 through 4, contains *S. neoabies*, *S. abies*, *R. pseudoumbilica* but lacks *D. asymmetricus* and any members of *Amaurolithus*. Thus this interval is placed in the *Sphenolithus neoabies* Subzone (CN11a). Samples 542A-1-5, 58–59 cm, 542-1,CC, and Core H2, Section 1 through 2, Core Section 4 are placed in the *Ceratolithus rugosus* Subzone (CN10c). *A. delicatus* last occurs in Sample 542A-H2-2, 67–78 cm. Samples 542A-H2-5, 69–70 cm and 542A-H2-6, 69–70 cm contain *C. acutus* and are placed in the *Ceratolithus acutus* Subzone (CN10b). Sample 542A-H2,CC is poorly preserved and contains no diagnostic forms.

Cores 2 through 10 are barren or have poorly preserved assemblages. Only Core 2 is entirely barren. All these cores are upper Miocene. *A. primus* is not found in any of the samples from these cores. It is believed that this is because that datum (base CN9b) was never reached, and not because of poor preservation. *D. surculus*, which is a marker for the base of the *Discoaster berggrenii* Subzone (CN9a), occurs sporadically throughout Cores 3 to 10. This occurrence is somewhat interesting in that *D. surculus* is one of the most solution-resistant species found in the Leg 78A sediments; and although it is found in many poorly preserved samples it is not found in several samples that have better preservation and contain placoliths. Therefore, if the occurrence

of *D. surculus* is not related to climatic changes, it is possible that two stratigraphic repetitions exist in the bottom of Hole 542. These repetitions would be between Samples 542A-9-3, 15–16 cm and 542A-9-2, 35–36 cm, and Samples 542A-5-5, 101–102 cm and 542A-5-4, 85–86 cm. Samples from Cores 3 through 10 containing *D. surculus* and *D. berggrenii* are placed in the *Discoaster berggrenii* Subzone (CN9a) based on the occurrences of those two species and absence of *A. primus*. Samples that do not contain any of these species and contain a useful assemblage of nannoplankton are considered slightly older. These samples are not assigned to specific zones because key species are not present.

Foraminifers

Hole 542

Most of the cored interval in Hole 542 contains frequent to abundant planktonic foraminifera assignable to the upper Miocene to the lower Pliocene.

Sample 542-1-2, 70–72 cm through Section 542-2,CC contain foraminifera representative of that part of Zone N19 (i.e., Pl1 of Berggren, 1973) below the extinction datum of *Globigerina nepenthes*. This interval is placed in Zone N19 below the extinction datum of *G. nepenthes* and above the first evolutionary appearance of *Sphaeroidinella dehiscens dehiscens*. Core 3 is dominated by common to frequent specimens of *G. nepenthes* and *Sphaeroidinellopsis subdehiscens paenedehiscens*. These sediments are assigned to the upper Miocene to lower Pliocene. The Miocene/Pliocene boundary is placed between Core 3, Sections 3 and 1 on the basis of the nannofossil data (see the preceding pages and Bergen, this volume). Core 4 contains a few planktonic foraminifera.

Hole 542A

The sediments from Hole 542A, Core 1 are assigned to that part of Zone N19 below the extinction datum of *Globigerina nepenthes* (i.e., Pl1 of Berggren). Cores 2 to 10 are all barren of foraminifera.

Radiolarians

No radiolarians are preserved in sediments cored at Site 542.

PALEOENVIRONMENT

Sediments of Holes 542 and 542A were deposited close to or below the CCD and thus contain specimens of only the most resistant species (e.g., *Globigerina nepenthes* or *Sphaeroidinellopsis subdehiscens paenedehiscens*).

ORGANIC GEOCHEMISTRY

The organic carbon and hydrocarbon contents of sediments cored in Holes 542 and 542A reflect the same trends that were observed at nearby Site 541. Organic carbon content ranges from 0.13 to 0.06% over the interval from 80 to 310 m. C₁ to C₆ hydrocarbon estimates ranged from 40 to 180 standard gas volumes per 10⁹ sediment volumes.

PORE FLUID CHEMISTRY

Six samples were taken for pore fluid chemistry, three apiece from Holes 542 and 542A. The data are listed in Gieskes et al. (this volume), where they are plotted versus depth and summarized. The principal interest of these data is in their comparison with Site 541 data. At Site 542, there are less steep gradients of Mg^{2+} and Ca^{2+} in the upper 75 m of sediments than at Site 541, but there are extremely sharp gradients between 75 and 150 m in these cations to levels comparable to those at Site 541. Below this, concentrations of Mg^{2+} are unusually high, higher than at Site 541, although Ca^{2+} concentrations are comparable. Indications that fluid overpressures occur near the base of this site, based on heat flow and fluid pressure measurements, suggest that the unusual Mg^{2+} concentrations result from pore fluids that originated below the décollement and migrated into the sediments just above the décollement at the site. (For an alternate interpretation, see Gieskes et al., this volume.)

PHYSICAL PROPERTIES

The physical properties of cores recovered from Site 542 are virtually identical to the properties measured in cores from Site 541.

Sonic Velocities

An average of two ultrasonic velocity measurements were made on samples from each core (Table 4). The variation in compressional velocity throughout the entire site is extremely uniform and quite small. The fastest and slowest velocities are 1.643 and 1.551 km/s, respectively, differing by only about 6%. As can be seen in Figure 8, the increase in velocity down the hole is very slight, very gradual, and linear.

We converted the vertical components of sonic velocities to acoustic impedance, defined as:

$$z = \rho \cdot V_p$$

where density = ρ and vertical velocity = V_p . As can be seen in Figure 8, the average acoustic impedance at Site 542 is nearly constant and averages about 2.80×10^5 g/cm² s units throughout the site.

In order to describe the variations in velocity with depth, we calculated mean velocities for given depth increments as well as for the entire site (Table 5).

Porosity, Density, and Water Content

Plots of water content, porosity, and density are shown in Figure 9. The density increases gradually with depth until a sub-bottom depth of about 240 m, below which the density decreases slightly, averaging about 1.75 g/cm³ to the bottom of the hole.

Surprisingly, the water content and porosity values increase slightly with depth at Site 542. The slight increase in water content at depth may be related to the excess pore water pressure encountered at the bottom of the hole.

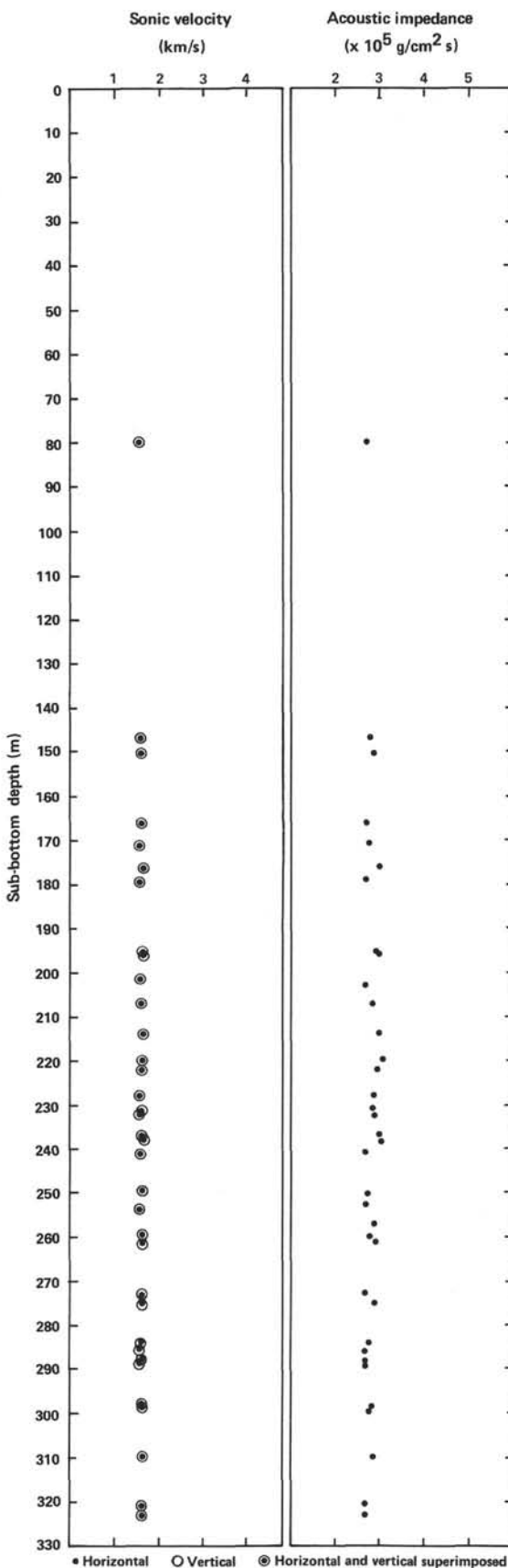


Figure 8. Plot of acoustic impedance and sonic velocity versus depth at Hole 542A. (Sonic velocities are calculated from recovered core samples and are *not* corrected to *in situ* values.)

Table 4. Summary of physical properties for Site 542.

Sample (core-section, interval in cm)	Sub-bottom depth (m)	2-min. GRAPE										Shear strength (kPa)	Thermal conductivity ($\times 10^{-3}$ (cal/ cm · s · deg))		
		Sonic velocity (km/s)		Wet-bulk density (g/cm ³)		Porosity (%)		Gravimetric			Acoustic impedance ($\times 10^5$ g/cm ² s)				
		H ^a	V ^a	H ^a	V ^a	H ^a	V ^a	Wet-bulk density (g/cm ³)	Porosity (%)	Water content (%)					
Hole 542															
H1-2, 31-34	80												44.5		
H1-2, 46-49	80	1.575	1.586	1.72	1.75	58.5	56.7	1.71	60.8	36.4	2.71		67.5		
H2-2, 72-75	147	1.573	1.562	1.91	1.77	47.2	55.5	1.76	58.4	34.1	2.75		>124.4		
H2-4, 73-76	150														
H2-4, 80-83	150	1.598	1.598	1.89	3.05	48.4		1.81	55.6	31.5	2.89				
H2-5, 21	151												2.828		
H2-7, 103-106	155												118.6		
H3-2, 62-64	195												>117.8		
H3-2, 64-72	195	1.621	1.618	2.07	1.91	37.6	47.2	1.79	56.4	32.2	2.90		>118.6		
H3-3, 32-35	196	1.621	1.623	1.96	1.93	44.2	51.9	1.85	53.0	29.4	3.00				
H3-3, 37-41	196												>116.1		
H3-4, 93-96	198												77.4		
1-1, 93-95	203														
1-1, 99-103	203	1.585	1.581	1.79	1.78	54.3	54.9	1.72	60.1	35.81	2.72				
1-4, 71-75	207	1.607	1.612	1.78	1.82	54.9	52.5	1.77	57.6	33.4	2.85				
1-4, 80-83	207												112.8		
1-5, 74-77	209												>145.0		
1-7, 36-38	211												120.2		
2-2, 112-115	214	1.628	1.636	1.94	1.92	45.4	46.6	1.85	53.7	29.8	3.03				
2-3, 119-121	216												116.5		
2-4, 88-91	217												>115.3		
2-6, 55-58	220												109.5		
2-6, 62-66	220	1.643	1.637	1.96	1.94	44.2	45.4	1.88	50.7	27.6	3.08				
2-6, 71	220												3.287		
3-1, 103-107	222	1.614	1.613	1.90	1.89	47.8	48.4	1.83	54.8	30.8	2.95				
3-1, 139-142	222												>122.7		
3-1, 63-66	225												105.4		
3-5, 98-101	228	1.593	1.596	2.57	1.87	7.8	49.6	1.77	58.5	33.8	2.82				
3-5, 104-106	228												85.7		
4-1, 55-59	231	1.619	1.602	1.91	1.82	47.2	52.5	1.77	56.6	33.9	2.84				
4-1, 61-63	231												117.8		
4-3, 85-88	234												>115.7		
4-5, 75-77	237												114.9		
4-5, 81-86	237	1.621	1.630	1.88	1.88	49.0	49.0	1.82	54.6	30.8	2.97				
4-6, 126-128	239												>112.8		
Hole 542A															
H1-2, 64-67	166	1.551	1.551	1.69	1.75	60.3	56.7	1.75	55.3	32.4	2.71		19.35		
H1-3, 50-53	168														
H1-5, 84-87	171	1.567	1.577	1.89	1.76	48.4	56.1	1.73	59.2	35.0	2.73				
H1-5, 124-127	171												>116.95		
1-2, 60-63	176	1.630	1.633	1.74	1.89	57.3	48.4	1.84	52.0	28.9	3.00				
1-2, 74-77	176												>120.25		
1-4, 65-68	179												116.13		
1-4, 133-136	179	1.569	1.558	1.68	1.73	60.9	57.9	1.72	59.9	35.8	2.68				
H2-1, 101-104	232	1.579	1.578	1.83	2.79	51.9		1.82	53.9	30.4	2.87				
H2-2, 91-94	233												>118.6		
H2-5, 127-130	238	1.621	1.620	1.93	1.87	46.0	49.6	1.85	52.4	29.0	3.00				
H2-6, 107-110	239												>118.6		
2-1, 111-114	241												120.2		
2-1, 118-121	241	1.578	1.570	1.77	1.74	55.5	57.3	1.70	62.3	37.6	2.67				
2-4, 34-37	245												>112.0		
2-7, 35-37	249	1.601	1.591	1.72	1.75	58.5	56.7	1.70	61.4	37.0	2.70				
2-7, 50	250												2.966		
3-3, 29-32	253												79.1		
3-3, 36-40	253	1.578	1.562	1.77	1.74	55.5	57.3	1.70	61.6	37.1	2.66				
3-5, 95-98	257												>109.5		
3-5, 102-106	257	1.620	1.615	1.84	1.81	51.3	53.1	1.77	58.4	33.8	2.86				
3-6, 43-46	257												>114.9		
4-1, 141-144	260	1.606	1.601	1.76	1.74	56.1	57.3	1.74	59.3	34.8	2.79				
4-2, 26-30	261	1.639	1.624	1.87	1.81	49.6	53.1	1.79	57.7	33.0	2.91				
4-2, 34-37	261												115.3		
4-3, 95-97	263												110.4		
5-3, 100-103	273												>112.0		
5-3, 108-112	273	1.596	1.622	2.01	1.48	41.2	72.8	1.64	71.2	44.6	2.66				
5-5, 23-25	275												135.9		
5-5, 29-33	275	1.640	1.637	1.45	1.71	74.6	59.1	1.76	59.8	34.8	2.88				
5-7, 22-25	278												115.3		
5-7, 45	278														
6-2, 113-115	281												106.7		
6-4, 97-101	284	1.611	1.593	1.75	1.80	56.7	53.7	1.73	61.3	36.3	2.76				
6-4, 105-108	284												60.9		
6-6, 51-53	286												85.7		
6-6, 58-62	286	1.581	1.601	1.69	1.69	60.3		1.67	64.1	39.3	2.67				
7-1, 106-109	288												82.4		
7-1, 132-135	288	1.609	1.589	1.75	1.74	56.7	57.3	1.69	62.3	37.7	2.69				
7-2, 12-15	289	1.584	1.573	1.02	1.69	10.0	60.3	1.68	62.8	38.3	2.64				
7-2, 18-21	289												52.7		
8-1, 109-112	298	1.615	1.613	1.76	1.79	56.1	54.3	1.74	59.4	35.0	2.81				
8-1, 119-123	298												90.6		
8-2, 3-6	299														
8-2, 8-12	299	1.626	1.640	1.75	1.78	56.7	54.9	1.71	62.0	37.1	2.80				
8-5, 19-22	303												102.1		
9-3, 29-32	310	1.630	1.634	1.78	1.81	54.9	53.1	1.76	58.2	33.8	2.88				
10-4, 25-28	321	1.610	1.580	1.56	2.13	68.1	34.0	1.67	63.9	39.3	2.64				
10-5, 74-77	323	1.627	1.598	1.74	2.14	57.3	33.4	1.72	60.0	35.7	2.75				
10-5, 99-102	323												>112.8		

Note: Some shear strength measurements exceeded instrumentation limits and are indicated by a greater than (>) symbol. These values are not plotted in any figures and are considered below failure strength of the material.

^a H = horizontal, V = vertical.

Table 5. Average sonic velocities: Site 542, Holes 542 and 542A.

Sub-bottom depth range (m)	\bar{V}_{\parallel} (km/s)	S	N	\bar{V}_{\perp} (km/s)	S	N
0-100	1.575		1	1.586		1
100-200	1.595	0.038	8	1.590	0.032	8
200-300	1.610	0.023	24	1.606	0.023	24
300-400	1.622	0.011	3	1.604	0.027	3
Total 0-323	1.605	0.024	36	1.591	0.067	36

Note: \bar{V}_{\parallel} = average velocity presumed parallel to bedding and perpendicular to the core; \bar{V}_{\perp} = average velocity presumed perpendicular to bedding and parallel to the core; S = standard deviation; and N = number of samples.

Shear Strength

Shear strength values for cores from Site 542 are listed in Table 4 and are shown in Figure 9. Although there is some scatter in the data, shear strength values are generally constant or decrease slightly down the holes at Site 542. The fairly uniform average values of shear strength suggest that the cored strata at Site 542, like those cored in the lower part of Site 541, have reached a maximum strength, perhaps due to consolidation from either overburden pressure or tectonic deformation or both.

Thermal Conductivity

A total of four conductivity measurements were made at Site 542 (Table 4). All four measurements are nearly the same, averaging about 3 mcal/cm · s · deg.

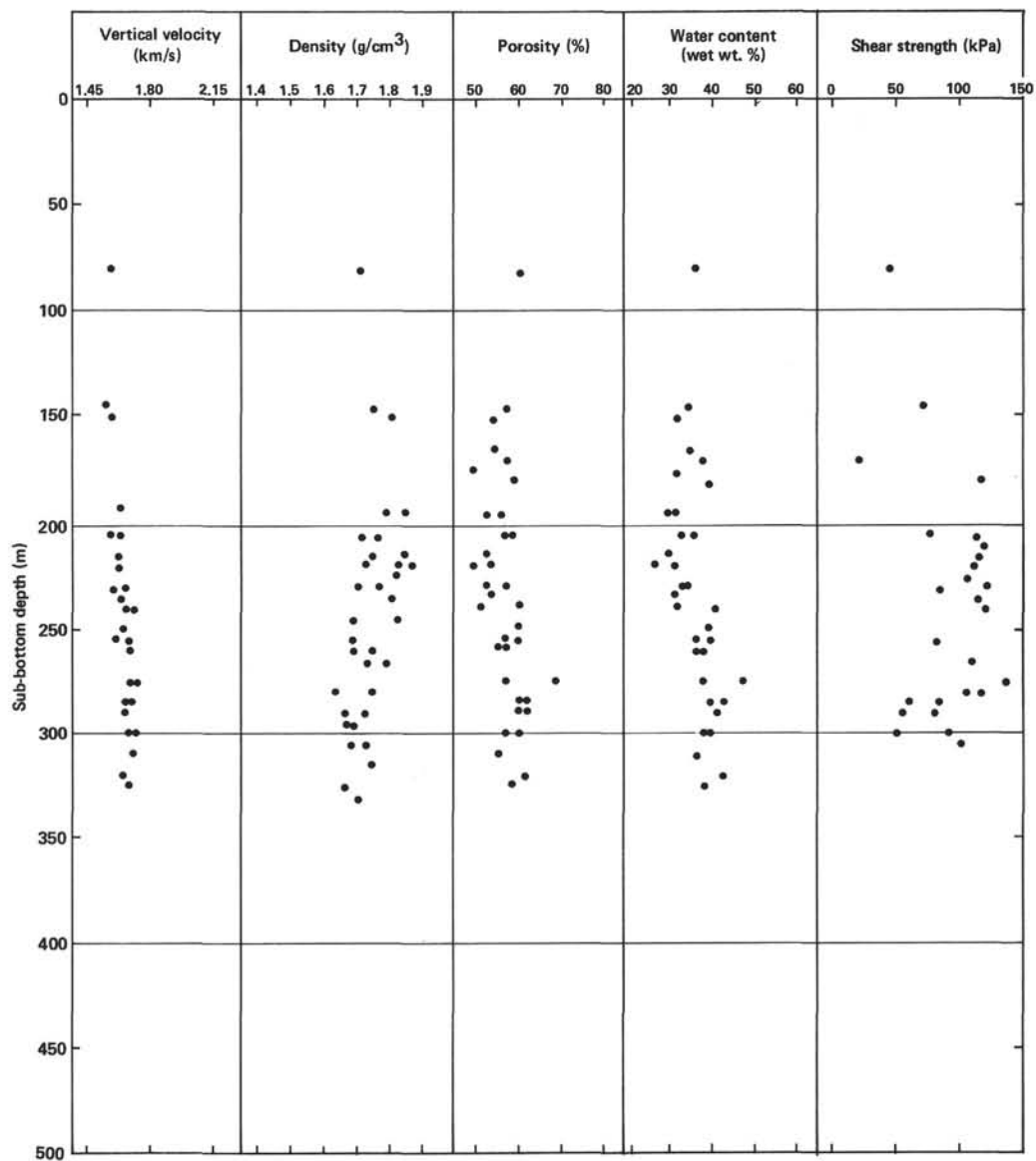


Figure 9. Plot of water content (wet wt. %), porosity (%), density (g/cm^3), vertical velocity (km/s), and shear strength (kPa) values versus depth at Site 542.

Some Related Findings

Figure 10 is a plot of porosity versus density measurements from cores taken at Site 542. Except for a few scattered points, most of the data plot as a linear function, very close to the empirically derived equation from DSDP relating density and porosity.

$$\rho_b = 2.70 - 1.675 \phi$$

where ρ_b = wet bulk density of a sample and ϕ = porosity of a sample.

As is true of Site 541, the rather uniform nature of the physical properties measured at Site 542, including sonic velocities, densities, porosities, acoustic impedances, and so on, is rather surprising. Earlier, we speculated that one explanation for the uniform behavior of strata here in a so-called subduction zone could be found in the *in situ*, interstitial pore fluids within the subduction complex. These overpressurized fluids, we speculated, could be absorbing the tectonic "shock" of overburden pressure as well as lateral motion from the underthrusting Atlantic Plate. Indeed, at the bottom of Hole 542B we did encounter pore water along a fault zone that may have been overpressured by some 300 to 350 psi. These excess pressures, measured on the ship, are sufficient to "float" the overburden drilled at Site 542 over a well-lubricated thrust zone. Such a localized high-pressure zone may confine lateral compression effects to narrow zones of deformation (along thrust planes), facilitate in the subduction and accretionary

processes, and explain the uniform physical properties of the strata cored at Site 542.

THE INADVERTENT PACKER EXPERIMENT

The stuck casing at Site 542 apparently resulted in isolating the hole below about 300 m and enabled us to make direct, through-the-pipe measurements of bottom-hole pressures (Fig. 4). The following comments stem from analysis of the pump pressure records and discussions with Glen Foss, Cruise Operations Manager, and Dave Billington, Driller.

Observations

According to Dave Billington the initial sticking occurred at 0423 hr. with a slight increase in pump pressure (~200 psi) but with continuing good circulation. Pumping was maintained for 4 min. at approximately 50 strokes/min. during which 1600 gallons were injected. Part of the pumped water could have escaped around the casing had it not been completely sealed off, and part may have entered the formation. According to the driller, water flowed freely out of the pipe during a connection at 0426 hr., after which the pressure rose to 300 to 350 psi, before the pump was started. This pressure increase is the best indicator of true formation pressure, as only a minimal volume of water could have been injected.

Another indicator of high formation pressure occurred from about 0517 to 0544 hr., when the pressure remained at a constant 300 psi while the driller attempt-

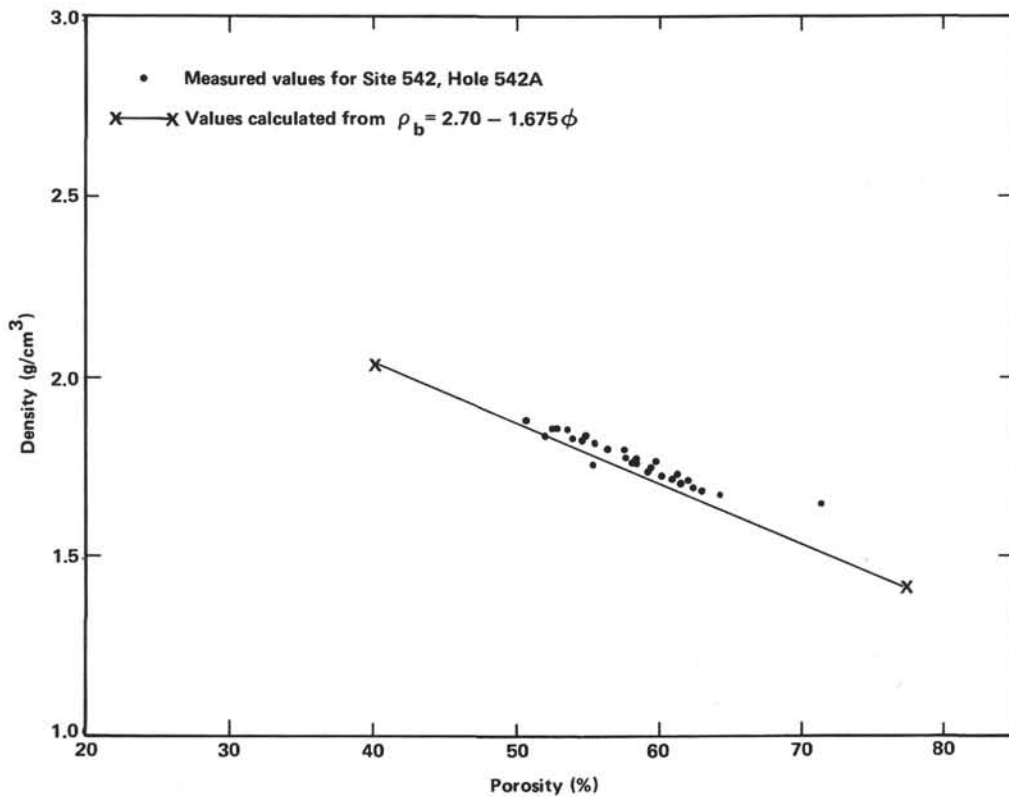


Figure 10. Plot of density versus porosity for core samples from Site 542. (See text for discussion.)

ed to release the drill string from the casing. Pumping of the release mechanism down the pipe took place from about 0430 to 0517 hr., introducing about 7400 gallons of fluid into the hole. Between 0500 and 0517 hr., a pressure of 400 psi was maintained due to pumping at a low rate.

We noted another interval of high formation pressure from 1054 to 1130 hr. Prior to 1054 hr. about 40,000 gallons of fluid had been pumped into the formation, with no resistance other than that required to overcome a back pressure of about 350 psi. At 1054 hr. The pump was shut off and the pressure immediately dropped to 350 psi. From 1040 to 1130 hr. the pressure slowly decreased to 300 psi, then dropped sharply to 0 when a relief valve was opened. After closing of the relief valve, the pressure continued to drop to 200 psi and then increased slightly to 240 psi at 1130 hr. Glen Foss attributed the slow decrease in pressure to progressive loosening of the line wiper.

We noted a final indicator of formation pressure just prior to firing the severing charge that ruptured part of the bottom-hole assembly. After pumping 48,000 gallons into the formation over 119 min., we shut off the pump at 1725 hr. and the pressure immediately fell to about 320 psi. The pressure decreased slowly from 320 to about 270 psi over 10 min., due to leaking around the line wiper, and remained at the latter pressure for 28 min. At 1803 hr. detonation of the severing charge pierced the pipe just above the casing, causing the pressure to drop to 0 at the drilling console.

Interpretations

Overall the foregoing observations suggest, but do not prove, the presence of excess fluid pressure at the base of Hole 542B. The salient interpretive points are: (1) The initial rise in pressure to 350 psi, shortly after sticking and minimal pumping into the formation, suggests that the recorded pressure is truly representative of the formation and not an artifact of injection of large amounts of water into a permeable isolated layer. (2) The ability of the formation to absorb water at more than 480 gallons/min. (60 strokes/min.) without pressure increase suggests it is very permeable. Moreover, the formation must be of large volume to have absorbed the substantial quantity of water injected. (3) The pressure drop after the severing charge was fired confirms the casing-drill pipe was a closed system while the excess pressures were recorded. (4) The maximum documented formation pressure was about 300 to 350 psi. Lower values probably reflect bleeding-off of pressure, probably around the line wiper. (5) The maximum observed pressure is approximately lithostatic. The maximum pressure the formation can withstand is lithostatic pressure plus the strength of the rock in tension (which is low). Therefore, regardless of the volume or pressure of water pumped into the formation, the return flow could only be slightly above lithostatic.

PALEOMAGNETICS

Objectives and techniques for paleomagnetic sampling at Site 542 were identical to those for Site 541. The

sampling was quite limited by the supply of reliable indicators of bedding. Twenty-six total samples were collected, eleven at beds dipping 10 to 35°.

In general, the samples are fairly stably magnetized, and horizontal magnetizations are rare, thus the individual polarity determinations are rather good. The measurements are tabulated in the chapter on paleomagnetism by Wilson (this volume). Inclinations are plotted in Figure 11. The primarily reversed interval in Hole 542, Cores 1 to 3, probably correlates to the Gilbert Epoch, consistent with nannofossil dates (Fig. 7). The mixed polarity interval in Hole 542A, Cores 2 to 4, probably correlates to the interval from polarity epochs 5 to 7, but control is poor here. No samples were taken below Core 4.

The structural interpretation, using the same techniques described in the Site 541 report, showed good internal consistency. Table 6 and Figure 12 summarize these attempts to determine the *in situ* strike and down-dip direction. The samples from Hole 542, Cores 3 and 4, were not used in this analysis because of the 7.6° deviation of the hole from vertical (see Operations section). As was the case for Site 541, the down-dip directions scatter over less than 180°, the favored direction here being to the east. The observation that beds seem

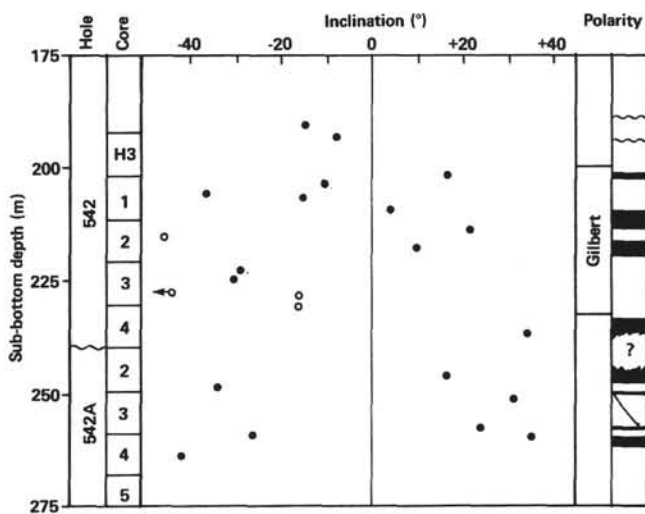


Figure 11. Stable magnetic inclination versus sub-bottom depth, and polarity interpretation. (Black areas indicate normal polarity; white areas show reversed polarity. Open circles represent data judged to be less reliable than the data represented by filled circles. Open circle with arrow indicates datum that is off the graph.)

Table 6. Structural interpretation based on paleomagnetic data.

Sample (interval in cm)	Bedding (relative to core)		Magnetization (corrected for bedding)			Apparent <i>in situ</i>	
	Strike	Dip	Inclination	Declination	Polarity	Strike	Direction
Hole 542							
H3-1, 145-147	300°	25°	-14°	114°	R	354°	E
Hole 542A							
2-4, 132-134	300°	25°	16°	310°	N	350°	E
2-6, 76-78	300°	35°	-34°	167°	R	313°	NE
3-2, 25-27	340°	25°	32°	342°	N	358°	E
3-6, 72-74	0°	18°	24°	266°	N	94°	S
4-4, 108-110	40°	15°	-42°	209°	R	11°	E

^a R = reversed; N = normal.

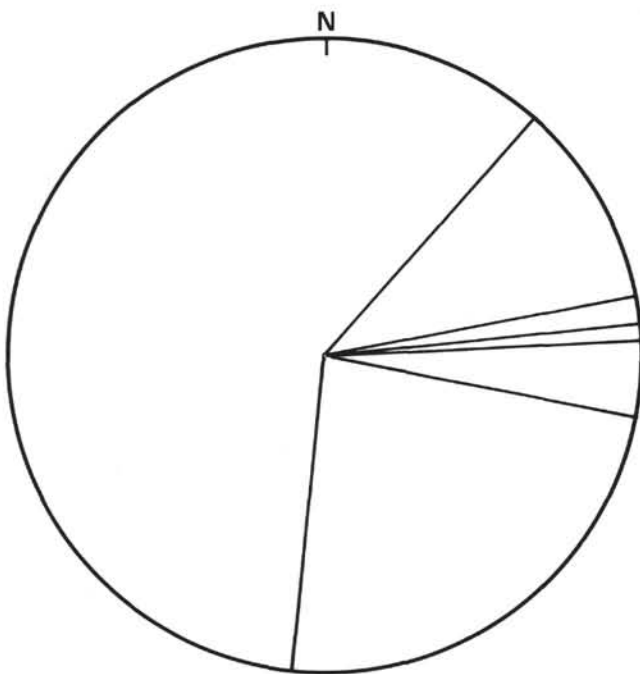


Figure 12. Inferred down-dip directions for dipping beds (from Table 6).

to dip in one general direction at each site again suggests monoclonal folding.

TEMPERATURE MEASUREMENTS

Temperatures were measured in the pipe in Hole 542B with the Gearhart-Owen logging tool down to approximately the depth at which the first severing charge that was dropped down the pipe ruptured the drill string.

Ambiguous results were obtained at this site. For more details, see Davis et al. (this volume).

SEISMIC STRATIGRAPHY—CORRELATION WITH LITHOLOGY AND PHYSICAL PROPERTIES

Seismic Stratigraphy

On profile A1D, at the location of Site 542, the seismic sequence is the same as the sequence previously described for Site 541, with minor changes in thickness (Fig. 3). Two units are defined. Seismic Unit 1 consists of 390 ms of discontinuously reflective material bounded by the seafloor above and Reflector 1 below. This first seismic unit extends to the bottom of the slope, about 1.5 km seaward of Site 542 and defines the toe of the Barbados Ridge complex. Poor acoustic seismic resolution does not allow us to define precisely the tectonic style of deformation along this profile. Seismic Unit 2 consists of 580 ms of a gently dipping sequence that rests on the deepest reflector, which in turn is presumed to be ocean crust (Reflector 3).

At Site 542, only the discontinuously reflective sequence was cored. In spite of discontinuous coring in the upper part of the section, the Pleistocene–Pliocene–upper Miocene sequence exhibits neither major lithologic nor sharp physical-properties boundaries (see previous discussion) that would yield impedance contrasts and resultant seismic reflectors. A similar situation occurs at Site 541 (see Site 541 report, this volume).

Using the value of 1.67 km/s (average of the velocity measurements—see Table 4) one can estimate that the last strata cored at 325 m in Hole 542A should correspond to the top of Reflector 1 (Fig. 13). Unfortunately, we could not sample below 325 m (beneath Reflector 1)

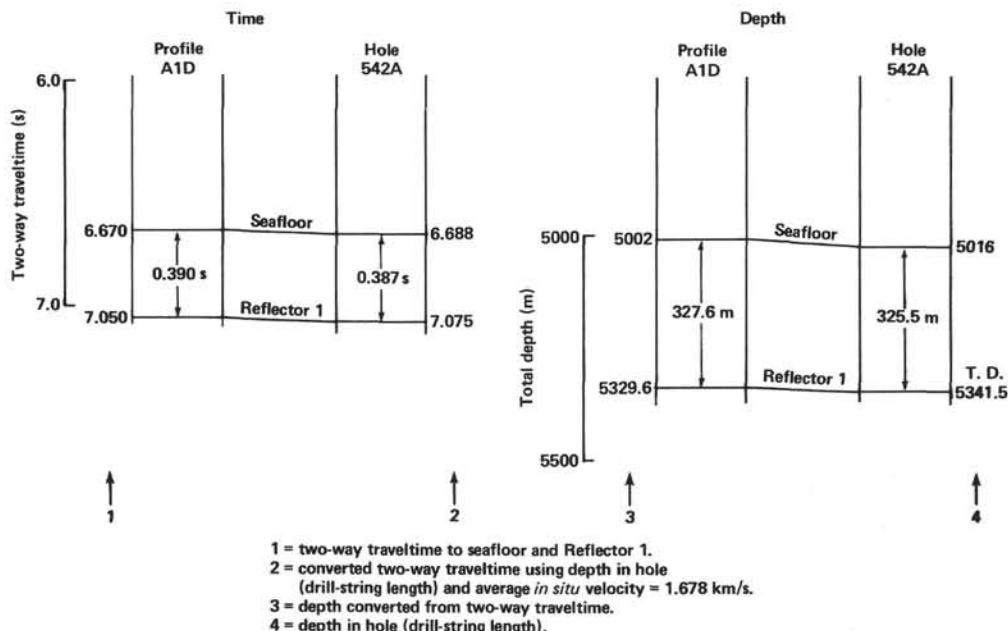


Figure 13. Correlations between seismic profile A1D and Site 542. T.D. = total depth cored—325.5 m.

to try and correlate with the lower Miocene radiolarian mudstones that presumably lie within or beneath Reflector 1 at adjacent Site 541.

SUMMARY AND CONCLUSIONS

At Site 542, in Holes 542 and 542A, after washing the uppermost part of the series, we cored, respectively, 52.56 and 90.22 m. The maximum sub-bottom depth is 325.5 m in Hole 542A. In spite of washed intervals on top of the two holes it is feasible to distinguish two units, ranging in age from Pleistocene to late Miocene.

From 250 m to total depth a zone of structural disruption with inclined bedding, highly disrupted strata, faults, polished slickensided surfaces, breccias, and scaly foliation suggests proximity of a major fault. As at Site 541, smectite is more abundant in this deformed interval. General deterioration in hole conditions and poor recovery reinforce the comparison. Drill-in casing was emplaced in this shear zone in Hole 542B in an attempt to prevent hole collapse; sticking of the casing resulted in an inadvertent packer test; recorded pressures in excess of 300 psi above hydrostatic pressure approximate the local lithostatic load and may facilitate underthrusting of the acoustically layered sequence. The absence of a major stratigraphic inversion suggests layer-parallel faulting (*décollement*) at the bottom of the hole. A slight increase in the water content and porosity probably reflects the excess pore-water pressure. This shear zone both here and at Site 541 correlates in depth with the boundary between the acoustically discontinuously reflective and layered sequences observed in the seismic records.

Unit 1 is composed of clayey calcareous and nannofossil-foraminifer ooze from 84.5 m to, respectively, 235.5 and 239.5 m in Holes 542 and 542A. Although ashy material is observed throughout the section, from 195.5 to 225 m in Hole 542, numerous bioturbated ash layers occur. This ash-rich, lower Pliocene to uppermost Miocene section is very comparable to Units 3 and 5 distinguished at Site 541. At Site 542 the conformable boundary between Units 1 and 2 is taken at the sharp decrease of CO_3Ca content. A repeated nannofossil zone between 183 and 195 m suggests minor reverse faulting.

Unit 2 from 239.5 to 325.5 m is made of generally greenish gray clayey mudstones with local layers of nannofossil oozes and ashy material. Bioturbation is common, especially in the lowermost part. At Site 542 Unit 2 is very similar to Units 4 and 6 of the superposed Tectonic Units A and B at Site 541. Two small repetitions of section may occur around 275 and 308 m (sub-bottom), from nannofossil indications.

The sediments cored at Site 542 accumulated in a hemipelagic to pelagic setting, and, as at Site 541, the lack of terrigenous turbidites suggests that the whole section was deposited either on a high (possibly the extension of Tiburon Rise) or on seafloor protected from terrigenous turbiditic influx. Local reworked foraminifers could indicate weak current action. Lithologic Unit 1 probably accumulated between the lysocline and CCD during the latest Miocene to the Pleistocene; deposition of Unit 2 occurred below the CCD in the late Miocene,

the sharp transition being observed near the Pliocene/Miocene boundary. Unfortunately, the lowermost part of the section is sparsely foraminiferous and cannot be exactly dated. The pelagic sedimentation was interrupted by occasional influxes of ash especially during the early Pliocene, as noticed at Site 541.

The greater thickness of Pliocene-Quaternary deposits at Site 542 exceeds that at Site 541 but does not necessarily indicate a higher rate of sedimentation (see Wright, this volume); rather a structural explanation may be more likely. A stratigraphic repetition could occur in the washed interval, as suggested by the small-scale inversion observed between Holes 542 and 542A. Also an inversion is suspected near the base of the hole.

The apparent deepening of the CCD inferred from younger sediments at Site 542 could be due to true depth variation of this surface or to vertical motions linked with the initiation of the offscraping.

Extremely low levels of C_2-C_6 hydrocarbons are consistent with the low content of organic matter in the sediment, comparable to Site 541 sediment.

Shipboard velocities from Site 542 cores are exceptionally uniform, suggesting penetration just through the discontinuously reflective sequence observed on the seismic profile. The velocity data suggest that Hole 542A penetrated close to Reflector 1 at the top of the acoustically layered sequence, which is apparently being underthrust.

Ignoring any minor stratigraphic inversions in the upper part of the section, we conclude that Holes 542 and 542A penetrated a single complete sequence, with high-angle dips below 200 m sub-bottom, overlying a highly tectonized zone with semipenetrative deformation. As such, the following conclusions may be drawn about the geometry of the toe of the accretionary prism (Fig. 14):

- 1) The main *décollement* occurs at the bottom of comparable lithologic units in Site 542 (Unit 2) and Site 541 (Unit 6). Thus the stratigraphic sequence cored at Site 542 can be compared with Tectonic Unit B at Site 541. The reverse fault occurring at Site 541 between Tectonic Units A and B is also located in a comparable lithostratigraphic sequence, indicating that the offscraping occurs at a peculiar stratigraphic level above the subducted sediments.

- 2) The contact between the acoustically chaotic and acoustically layered units, the shear zone of *décollement* observed on seismic records at the top of Reflector 1, is very gently dipping toward the west (less than 3°). But the high-angle dips observed in cores from both Sites 542 and 541 demonstrate disharmony between the off-scraped sediments and the acoustically layered sequence, as well as between the different offscraped packages within the discontinuously reflective unit, as suggested by observations at Site 541.

Unfortunately the casing emplaced to maintain the unstable zone at Hole 542B was stuck and did not permit us to pursue the hole through the major tectonic contact. Fluid overpressures were suggested by the increase of water content at depth and the inadvertent packer experiment monitoring high fluid pressures in

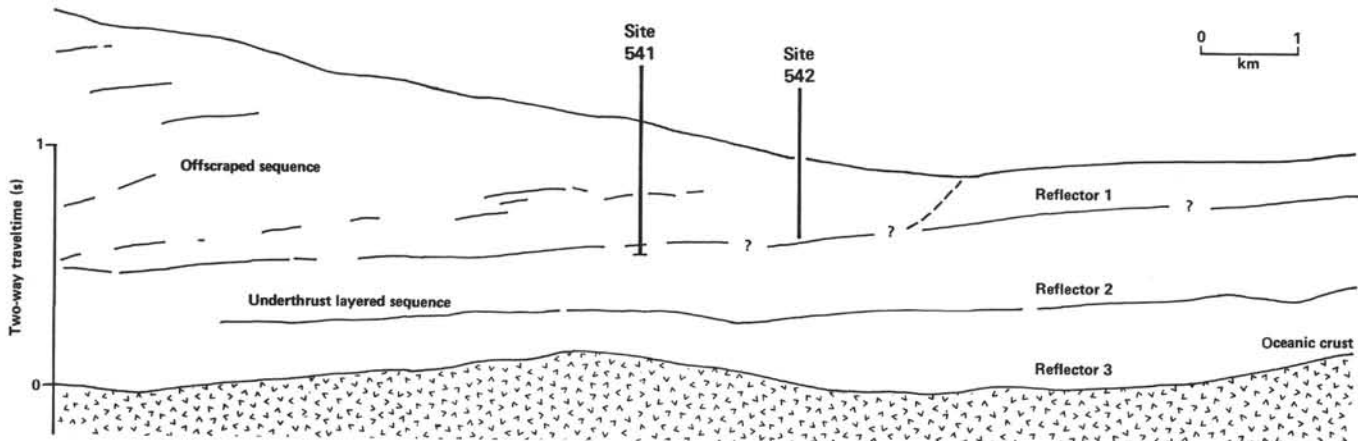
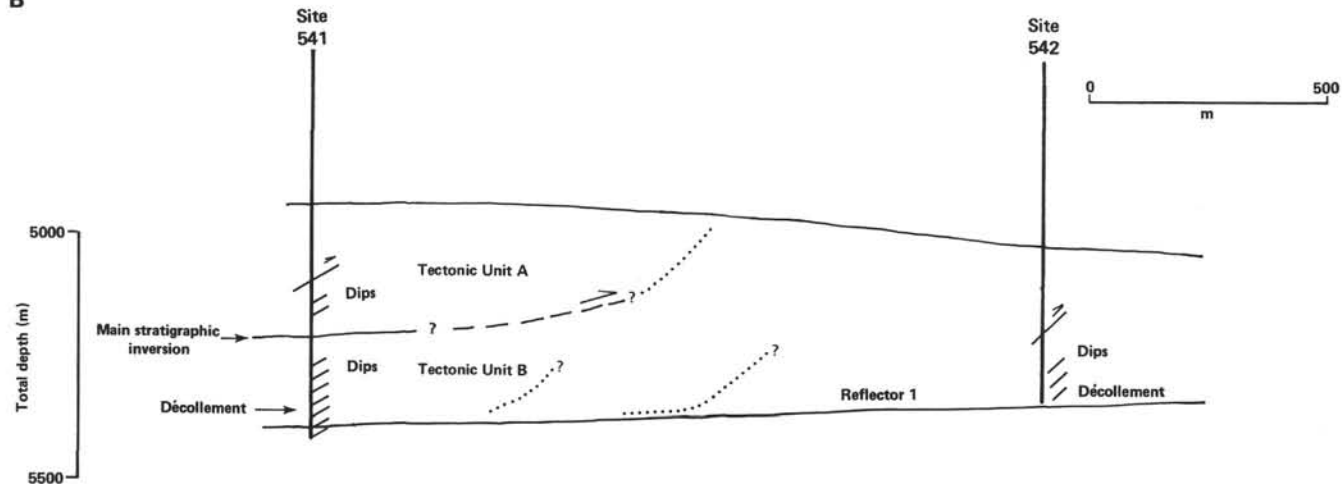
A**B**

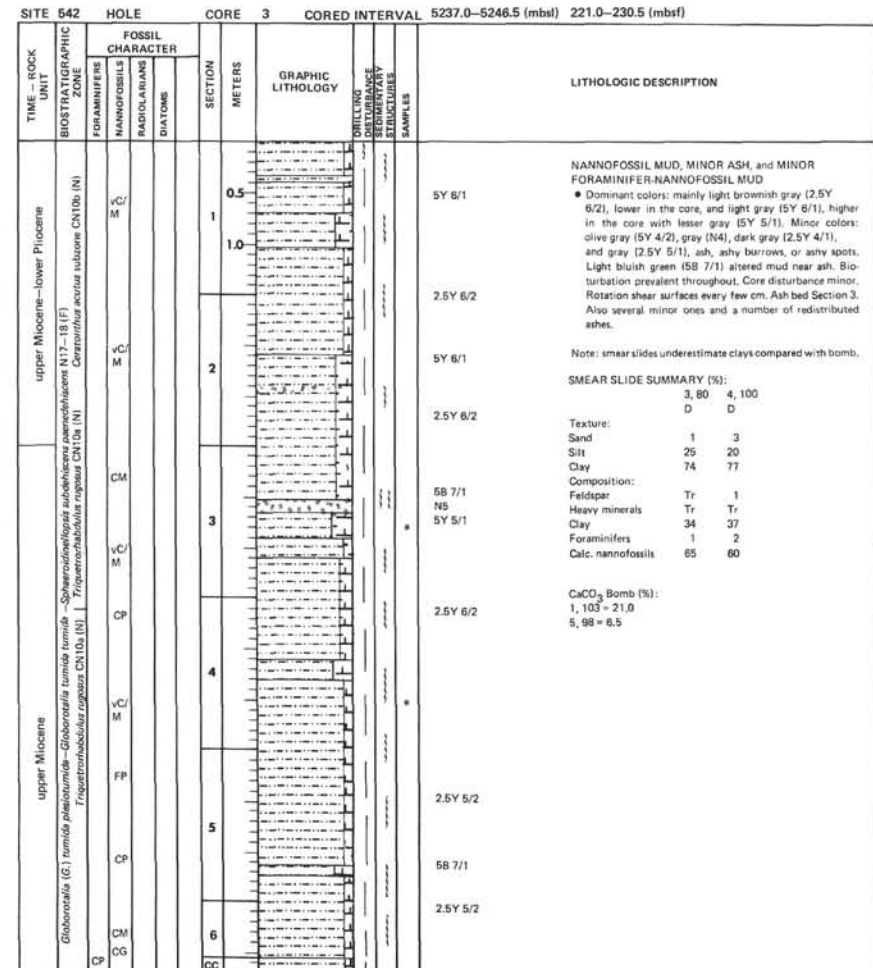
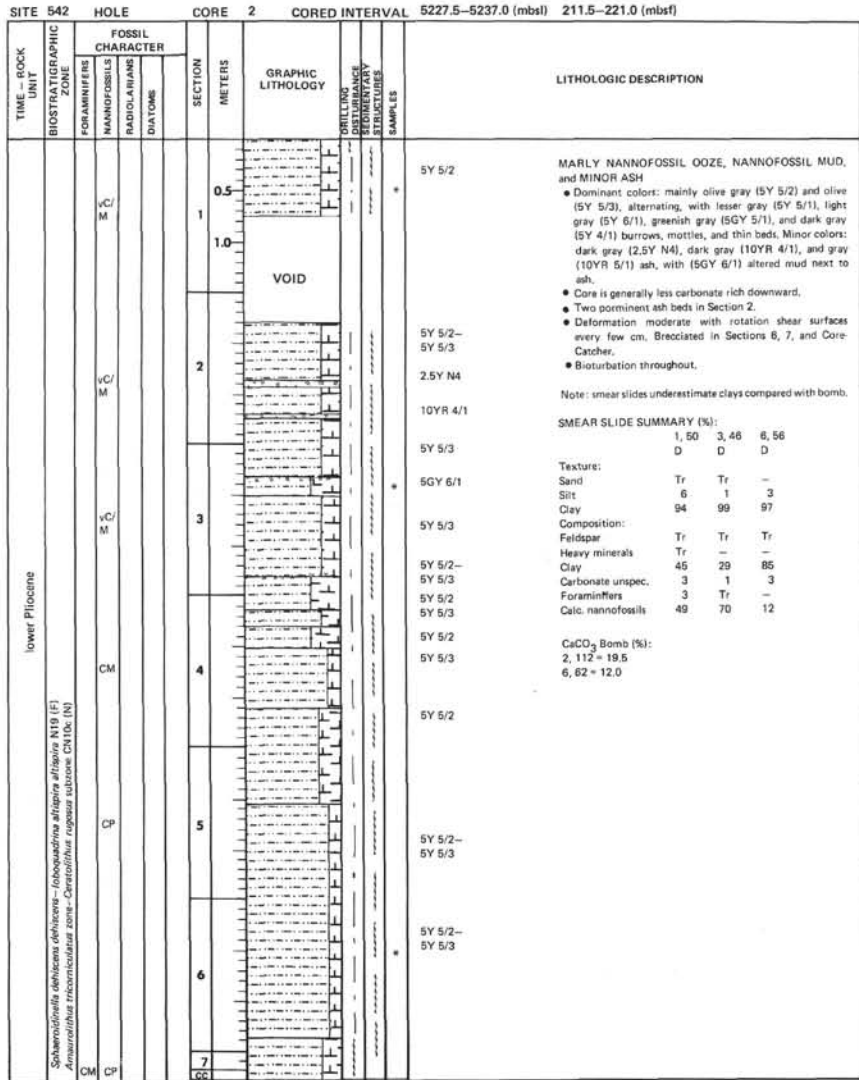
Figure 14. A. Comparison between interpretive cross-section from profile A1D (from Fig. 3) and B. data from Sites 541 and 542 illustrating the geometry of the off-scraped sequence.

the basal deformation zone. The fluid pressures undoubtedly facilitate the underthrusting of the acoustically layered sequence.

REFERENCES

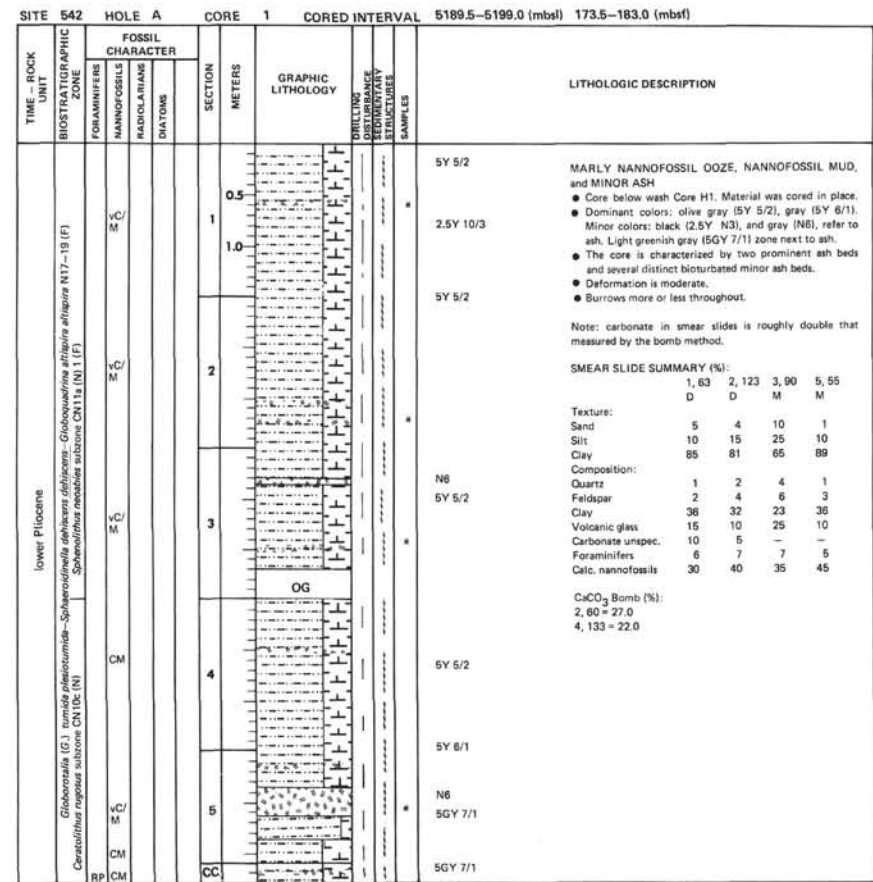
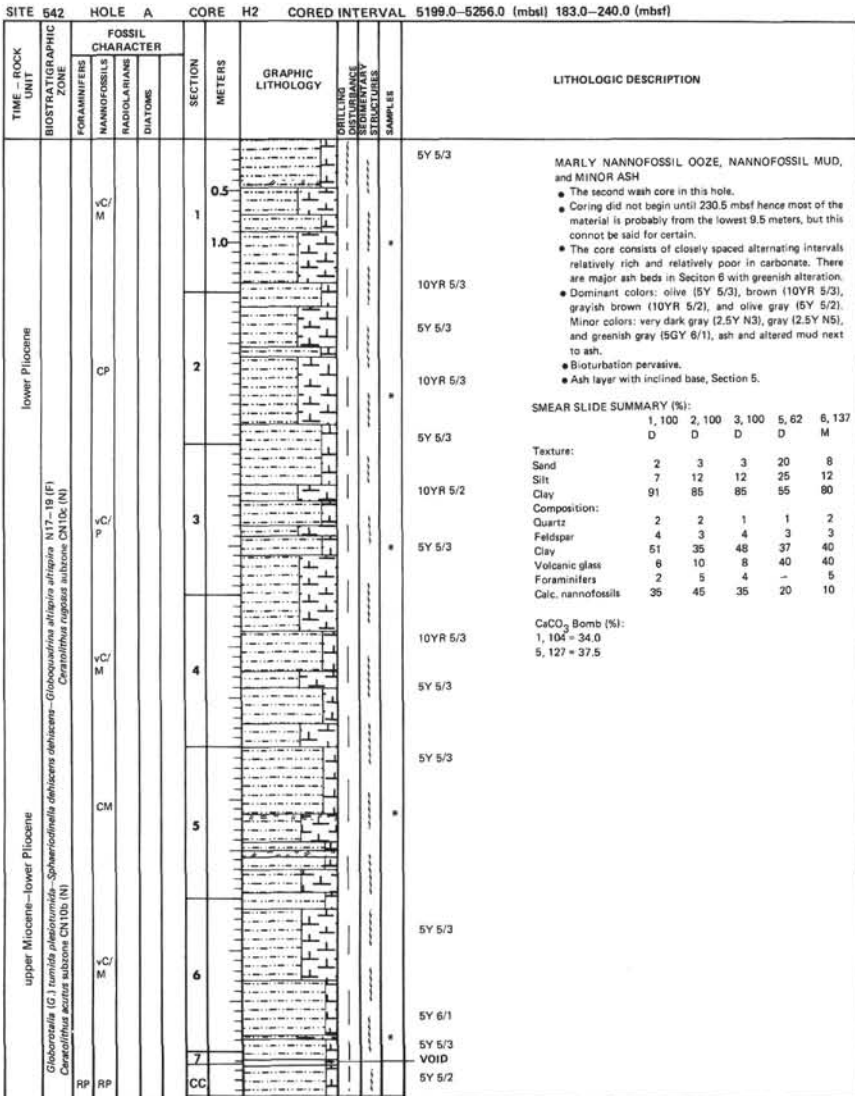
- Berggren, W. A., 1973. The Pliocene time scale: calibration of planktonic foraminiferal and calcareous nannoplankton zones. *Nature*, 243:391-397.
- Blow, W. H., 1969. Late middle Eocene to Recent planktonic biostratigraphy. In Bronnimann, P., and Renz, H. H. (Eds.) *Proc. First Int. Conf. Planktonic Microfossils*, Geneva, 1967, 1:199-422.
- Bukry, D., and Okada, H., 1980. Supplementary modification and introduction of code numbers to the low-latitude coccolith biostratigraphic zonation. *Mar. Micropaleontol.*, 5:321-325.
- Gartner, S., 1977. Calcareous nannofossil biostratigraphy and revised zonation of the Pleistocene. *Mar. Micropaleontol.*, 2:1-25.
- Gartner, S., and Bukry, D., 1975. Morphology and phylogeny of the Coccolithophycean family, Ceratolithacere. *J. Res. U.S. Geol. Surv.*, 3:451-469.

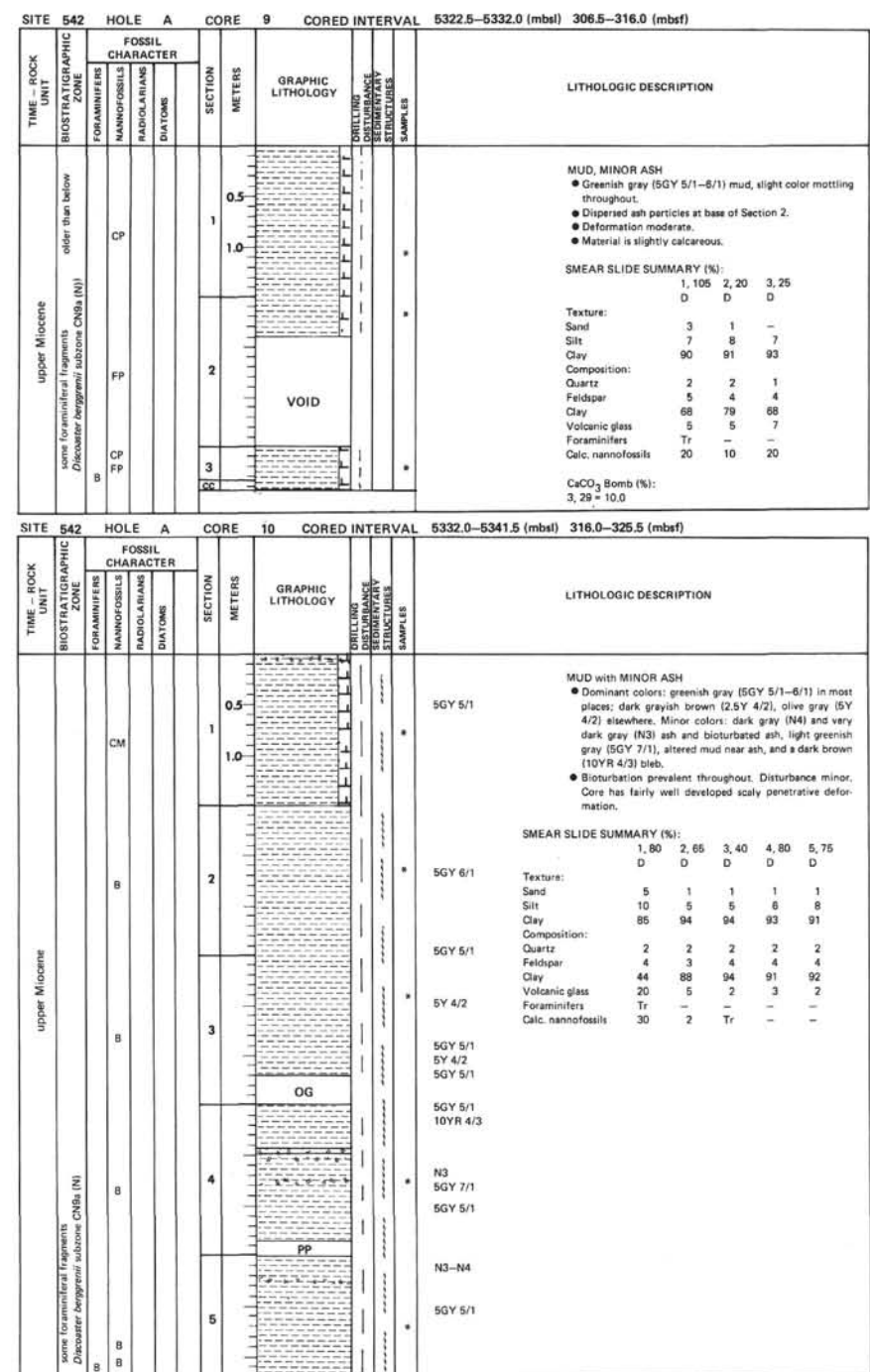
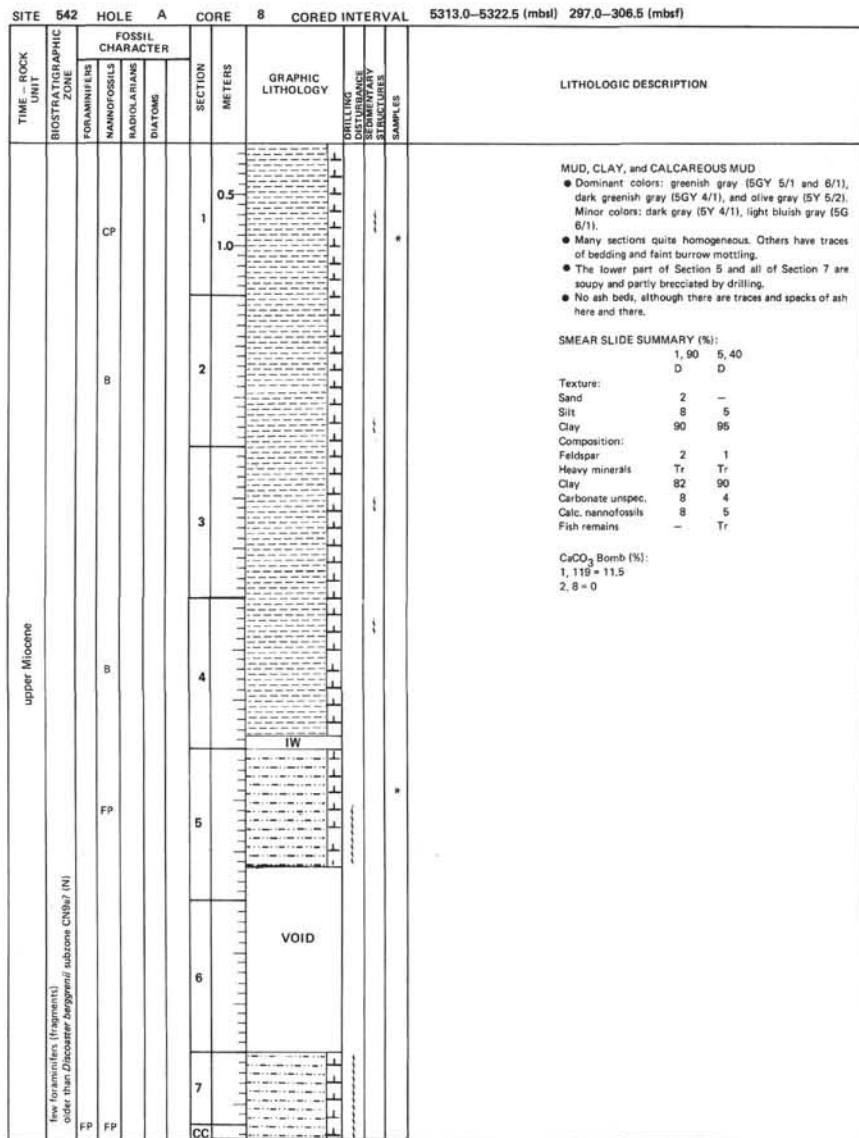
TIME - ROCK UNIT	SITE 542	HOLE	CORE	H1	CORED INTERVAL	5016.0–5104.0 (mbst) 0.0–88.0 (mbst)	
						FOSSIL CHARACTER	
BIOSTRATIGRAPHIC ZONE	FORAMINIFERS	MICROFAUNA	STRUCTURES	DRILLING METERS	DISTURBANCE BEDROCK STRUCTURES	SAMPLES	LITHOLOGIC DESCRIPTION
	NANNOFOSSILS	RADIOLARIANS	DIATOMS				
lower Pleistocene	Globorotalia truncatulinoides truncatulinoides N22 (F)	Cyathocerasites macriformis zone (N)	AG	CM	0.5	SY 5/3	MARLY NANNOFOSSIL Ooze and MINOR ASH
			CP	CM	1	SY 5/2	• Wash core. Material may have been recovered 0–88 mbst, but probably it was cored in the lowest 9.5 m, as indicated by the sediment age.
			CP	CM	1.0	SY 6/1	• Dominant colors: gray (SY 6/1), olive gray (SY 5/2), and olive (SY 5/3).
			CP	CM	1.5	SY 5/3	• Intensely disturbed, with large void between Sections 3 and 6.
			CP	CM	2	SY 5/2	SMEAR SLIDE SUMMARY (%):
			CP	CM	2.5	SY 8/1	1,90 1,116 2,60 6,19 D D D D
			CP	CM	3	SY 5/2	Texture: Sand 3 3 3 10 Silt 12 15 17 10 Clay 85 82 80 80
			CP	CM	4	SY 5/2	Composition: Quartz 2 4 2 2 Feldspar 5 6 5 5 Clay 25 20 20 18 Volcanic glass 7 10 15 10 Carbonate unsped. – – 5 – Foraminifera 10 8 8 10 Calc. nannofossils 51 53 45 55
			CP	CM	5	SY 5/2	CaCO ₃ Bomb (%): 2, 46 = 40.0
			CP	CM	6	SY 5/2	IW
			CP	CM	7	SY 5/2	CC

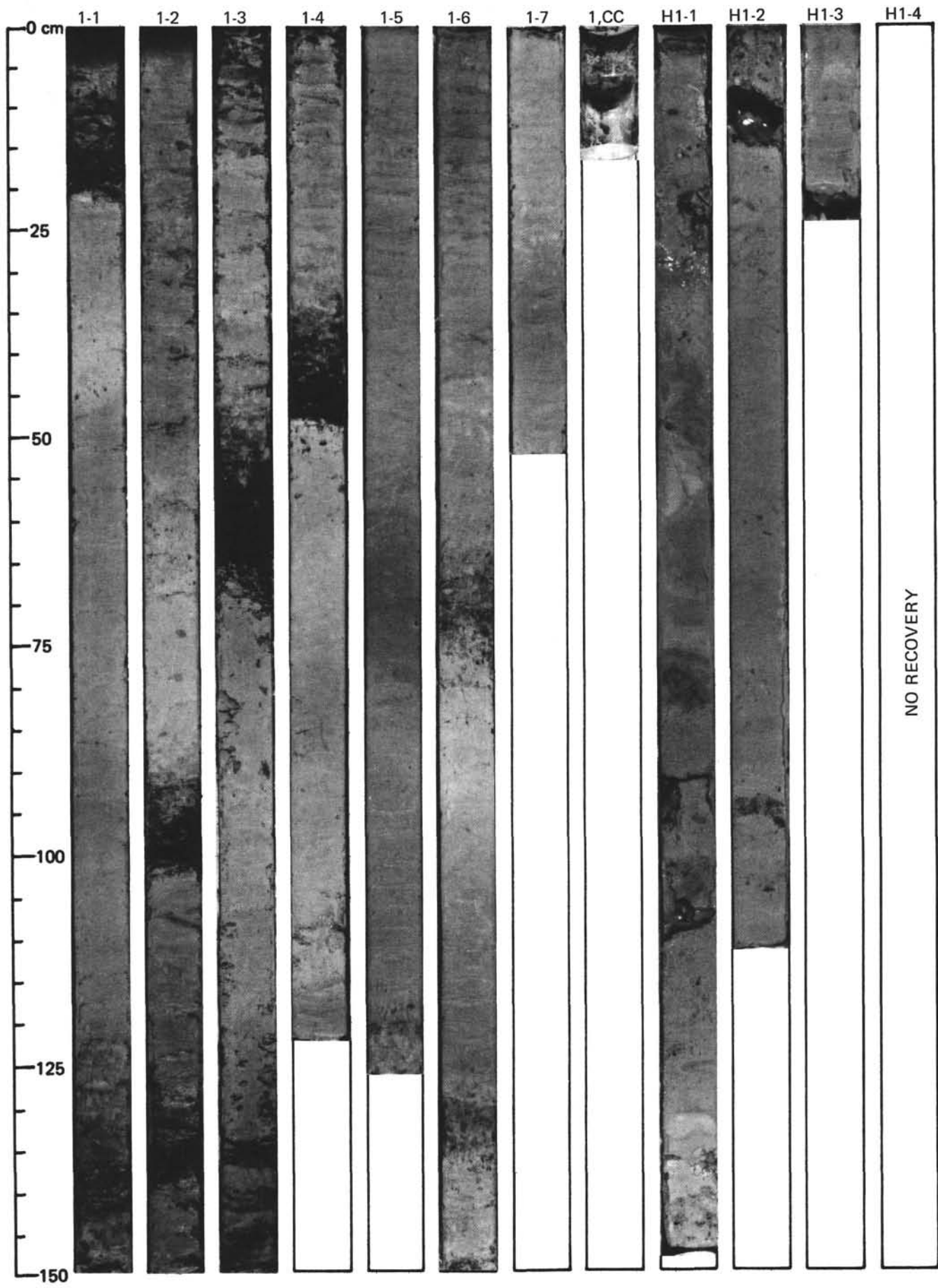


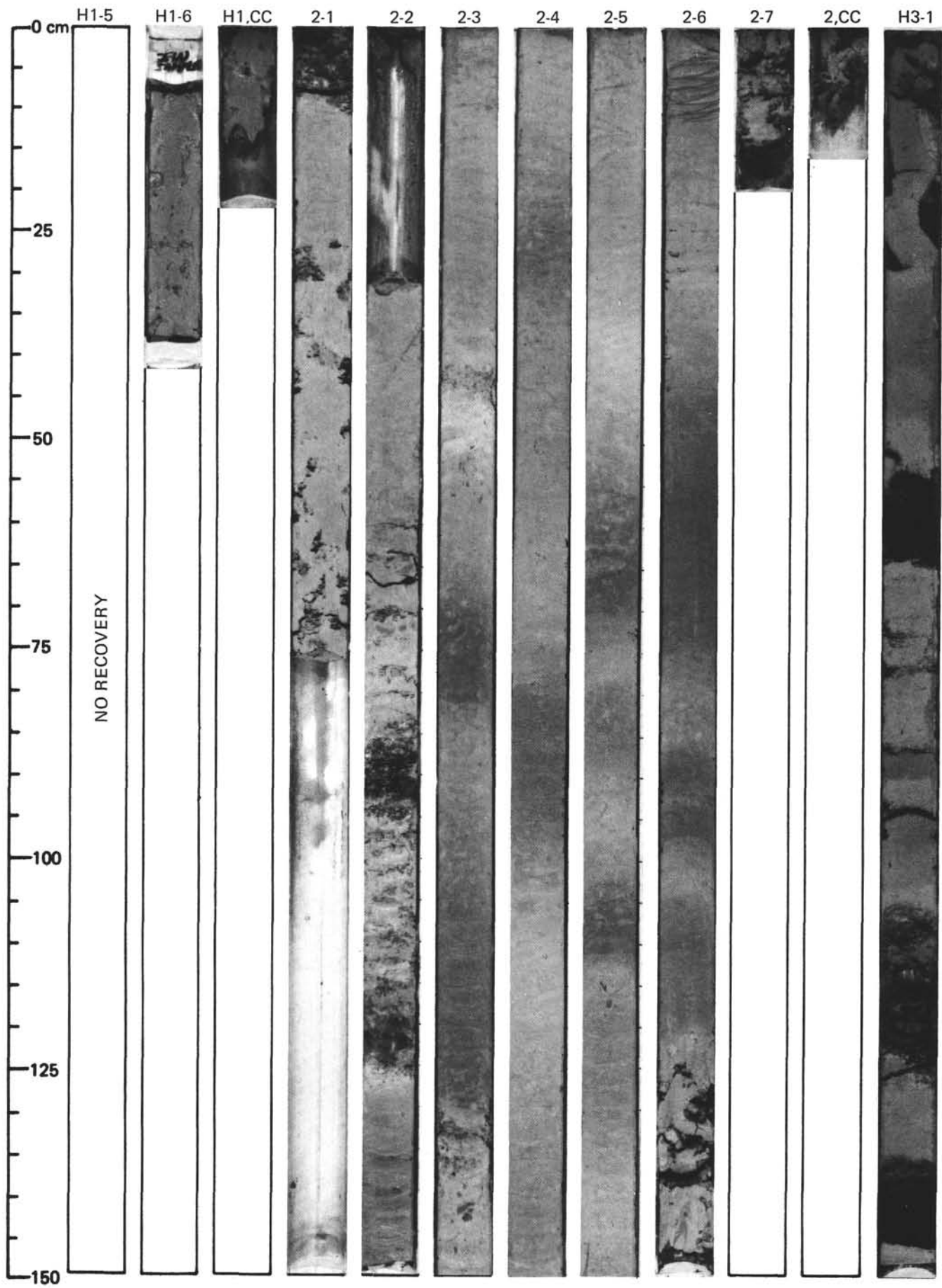
TIME - ROCK UNIT	SITE 542	HOLE	CORE 4	CORED INTERVAL 5246.5–5256.0 (mbsl)	230.5–240.0 (mbst)	LITHOLOGIC DESCRIPTION						
						FOSSIL CHARACTER	SECTION	METERS	GRAPHIC LITHOLOGY	DRAILLING DISTURBANCE STRUCTURES	SAMPLES	
BIOSTRATIGRAPHIC ZONE												
upper Miocene												
<i>Amarolinthus primus</i> subzone CRb6 (N)	B	FP	CP	OG	6	2.5Y 5/2– 5Y 5/2 10YR 5/2		0.5				
	B	CP	CP		7	5Y 5/2 5Y 4/1– 5Y 5/1						
				CC								

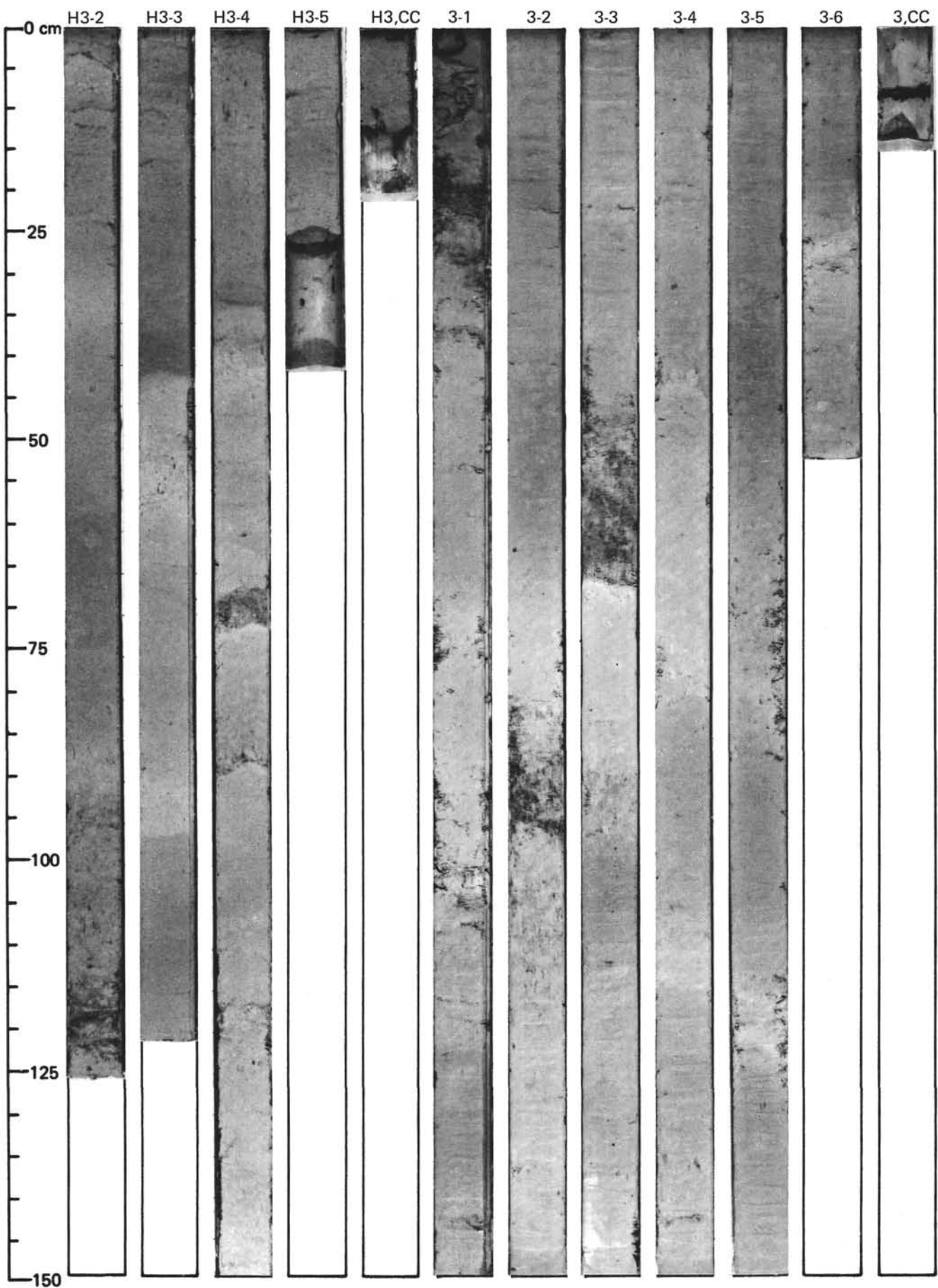
TIME - ROCK UNIT	SITE 542	HOLE	CORE H1	CORED INTERVAL 5016.0–5189.5 (mbsl)	0.0–173.5 (mbst)	LITHOLOGIC DESCRIPTION						
						FOSSIL CHARACTER	SECTION	METERS	GRAPHIC LITHOLOGY	DRAILLING DISTURBANCE STRUCTURES	SAMPLES	
BIOSTRATIGRAPHIC ZONE												
upper Pliocene												
<i>Sphaeroidinella delucensis</i> - <i>Globogaudnia affinis</i> aff. <i>affinis</i> N19 (F) <i>Diastoceraspis</i> subzone CN12a (N)	AM	CM	CM	CC	1	2.5Y 5/2– 5Y 5/2 10YR 5/2		0.5				
					2	5Y 5/1						
					3	5Y 5/1						
					4	5Y 6/2						
					5	5Y 6/2						



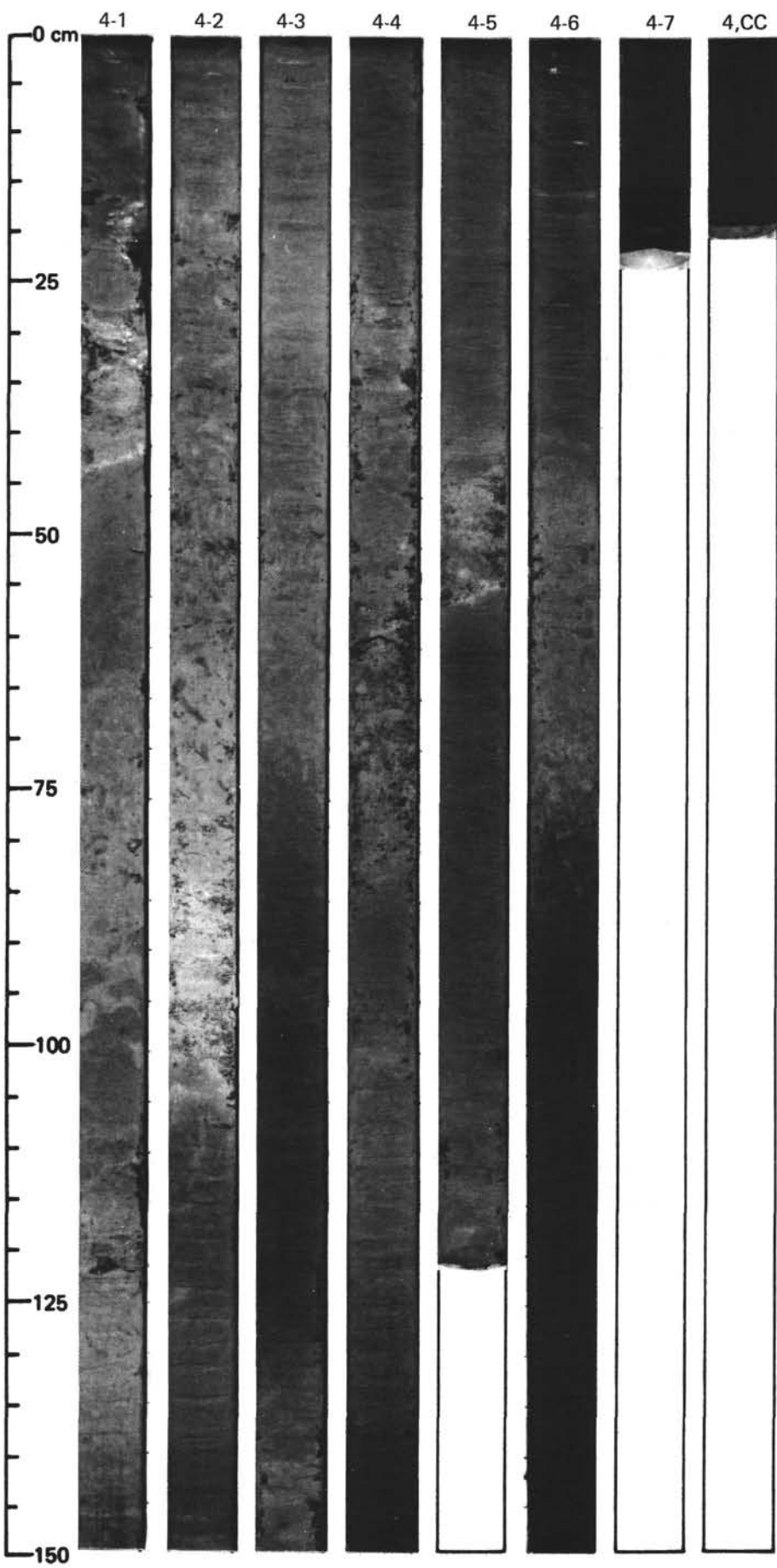


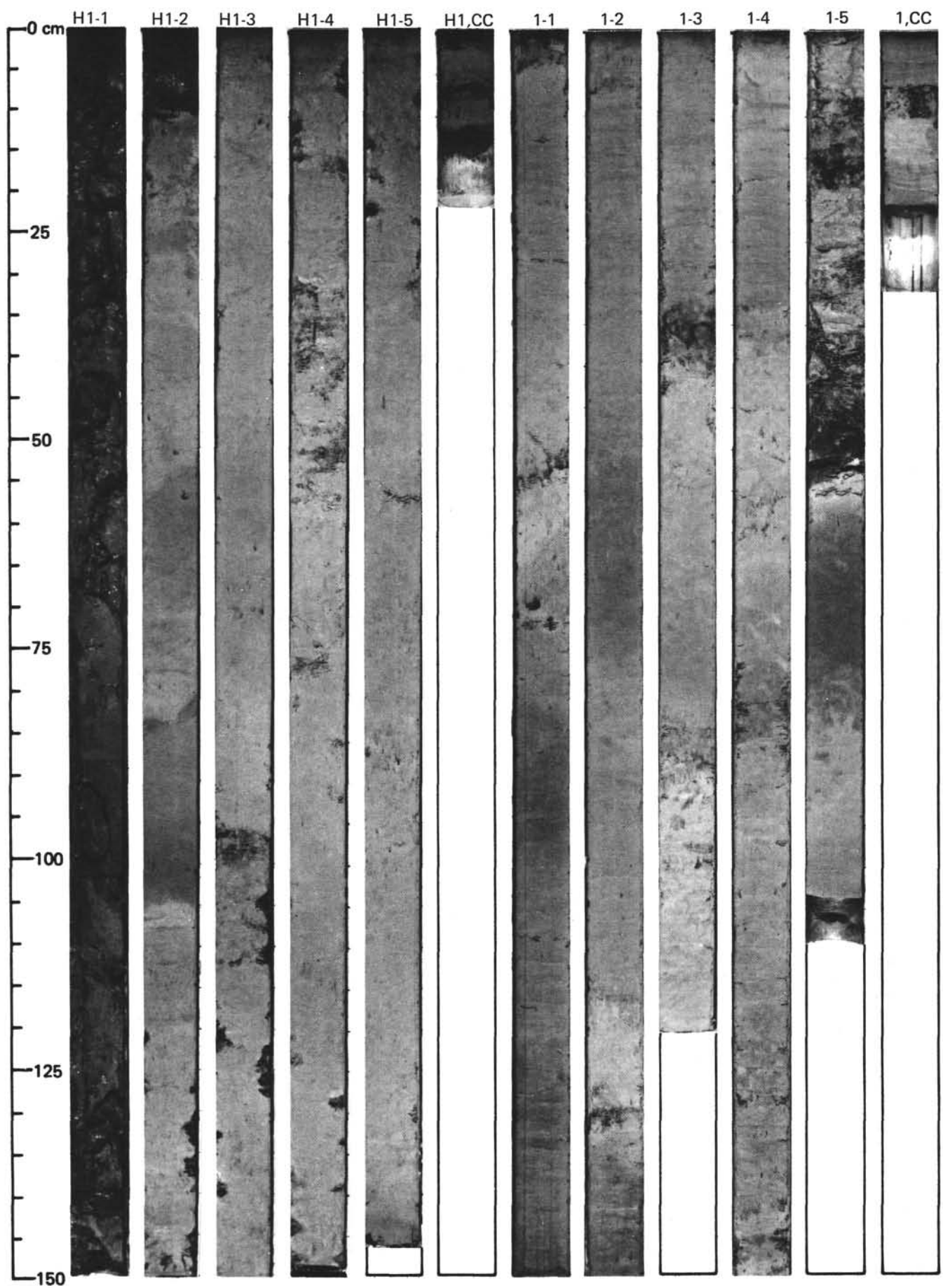






SITE 542





SITE 542

